

# Species diversity and stand structure as drivers of canopy complexity in southern African woodlands

John L. Godlee

1st September 2021

## Abstract

Atmospheric CO<sub>2</sub> enrichment and human-induced climate change are expected to drive woody encroachment and increased tree growth rates across African savannas, with consequences for ecosystem function, particularly related to carbon dynamics. The patch dynamics of savanna-woodland mosaics are complex however, as woody growth is mediated by seasonal fire that is itself driven by properties of the woody overstorey. It is unclear how variation in tree species composition and stand structure in this ecosystem affects woody canopy complexity, and how this might determine future vegetation dynamics. Here, I conducted a study of canopy structure in southern African savannas using terrestrial LiDAR, at sites in Bicuar National Park, Angola and Mtarure Forest Reserve, Tanzania, to explore relationships between tree species diversity, species composition, the spatial distribution of trees, variation in tree size and canopy complexity. Species diversity was found to have consistent weak positive effects on plot scale canopy complexity metrics related to canopy density, but a negative effect on metrics related to the spatial heterogeneity of canopy material distribution. Species diversity caused an increase in canopy height, canopy closure, and within-canopy structural complexity, together suggesting that diverse canopies may promote woody encroachment and exhibit higher upper limits on biomass. Stochasticity in neighbourhood scale stand structure partially weakened species diversity effects at small spatial scales. Finally, no strong effect of tree size variation on canopy complexity was found, but there was a clear effect of species diversity on canopy complexity, suggesting a decoupling of tree stem size and canopy foliage volume, highlighting species specific differences in the plasticity and physiological limits of crown shape.

## 1 Introduction

Atmospheric CO<sub>2</sub> enrichment, coupled with climate change and changing disturbance regimes, is expected to drive woody encroachment, i.e. proliferation of trees into previously non-wooded areas, and increased growth of trees in currently wooded areas, across the savanna biome over the coming century (Criado et al., 2020; Mitchard & Flintrop, 2013; Stevens et al., 2016). As atmospheric CO<sub>2</sub> concentrations increase, C<sub>3</sub> trees are expected to gain a competitive edge over C<sub>4</sub> grasses due to differences in photosynthetic pathway and carbon use efficiency (Buitenwerf et al., 2012), allowing trees to increase their productivity. This is expected to have cascading effects on canopy cover, grass growth, and disturbance regime (Bond & Midgley, 2012). If realised, woody encroachment and woody densification will have significant effects on the global carbon cycle, as more CO<sub>2</sub> is stored in woody biomass, as well as myriad other effects on ecosystem structure (Donohue et al., 2013). Indeed, tropical savannas have been identified as the fastest increasing component of the terrestrial carbon sink (Sitch et al., 2015). Previous studies however, have reported wide variation in rates of woody encroachment and densification (Mitchard & Flintrop, 2013), particularly in disturbance-prone savannas such as miombo woodlands in southern Africa (Axelsson & Hanan, 2018), and it is unclear how the fertilisation effect of atmospheric CO<sub>2</sub> enrichment interacts with other ecosystem properties to alter vegetation structure (Körner, 2017; Reich et al., 2014).

Savanna vegetation is defined by the coexistence of trees and grasses (Scholes & Archer, 1997).

42 In the tropical mesic savannas of southern Africa, disturbance by fire and herbivory are the main  
43 limitations on tree cover, preventing the competitive exclusion of shade-sensitive C<sub>4</sub> grasses  
44 where climatic conditions would otherwise allow for closed canopy forest (Sankaran et al., 2005).  
45 C<sub>4</sub> grasses also provide the main fuel source for seasonal fires in these savannas (Frost, 1996),  
46 producing a positive feedback where an increase in tree cover reduces grass fuel load, reducing  
47 fire frequency and intensity, increasing tree cover, and so on (Staver & Koerner, 2015). As such,  
48 even small perturbations in tree cover can lead to large changes in vegetation structure if critical  
49 thresholds of tree cover are crossed (Hirota et al., 2011). Previous research has sought to identify  
50 environmental factors which affect tree cover and its responses to atmospheric CO<sub>2</sub> enrichment,  
51 but few have considered the functional role of the existing tree community and its effect on  
52 ecosystem processes.

53 Canopy structure describes the spatial distribution and density of tree canopy foliage (Lowman &  
54 Rinker, 2004). Canopy structural complexity, i.e. the spatial heterogeneity of foliage distribution  
55 within the canopy, has been linked to increased net ecosystem productivity (Baldocchi & Wilson,  
56 2001; Chen et al., 2012; Gough et al., 2019; Hardiman et al., 2011; Law et al., 2001; Morin, 2015),  
57 increased resilience of productivity (Pretzsch, 2014), reduced understorey light penetration (Fotis  
58 et al., 2018; Scheuermann et al., 2018; Sercu et al., 2017), and greater moderation of understorey  
59 micro-climate (Wright et al., 2017). In temperate and boreal forests, functional differences among  
60 coexisting tree species in their vertical and horizontal canopy occupation provide a link between  
61 species diversity, canopy structural complexity and canopy density, with canopy complexity  
62 constituting a mechanism for positive biodiversity-ecosystem function effects observed in wooded  
63 ecosystems (Barry et al., 2019; Pretzsch, 2014). In tropical savannas, tree species diversity might  
64 therefore influence ecosystem-level woody thickening in response to elevated atmospheric CO<sub>2</sub>,  
65 where competition effects in diverse tree communities are reduced due to niche separation, and  
66 can more effectively increase foliage density and reduce understorey light penetration (Sercu  
67 et al., 2017), excluding grass and thus reducing both the likelihood and intensity of disturbance.

68 As well as the species diversity of trees, the spatial distribution and relative size of tree stems,  
69 i.e. stand structure, is also expected to affect canopy structural complexity (Stark et al., 2015).  
70 Heterogeneity in stem size, whether a result of species diversity, disturbance history or some  
71 other factor, is expected to increase canopy complexity and canopy density as individuals of  
72 different sizes occupy different parts of the vertical canopy space (Panzou et al., 2020), and  
73 may differ in light requirements (Charles-Dominique et al., 2018). Additionally, clustering of  
74 individuals in space is expected to increase canopy structural heterogeneity across the wider  
75 savanna landscape, but ultimately decrease total foliage density due to an increase in competitive  
76 interactions (Dohn et al., 2017). Clustering may occur as a result of disturbance history at  
77 local spatial scales (Groen, 2007; Schertzer et al., 2015), facilitation effects among individuals  
78 in stressful environments (Ratcliffe et al., 2017), due to other limitations on dispersion arising  
79 from growth strategy (Silva & Batalha, 2011), or from environmental heterogeneity (Getzin  
80 et al., 2008). More diverse communities may allow greater stem density and greater foliage  
81 density within clusters, as differences in canopy occupancy among species reduce negative effects  
82 competition among individuals on growth (Gough et al., 2019).

83 Functional differences among floristic types of savanna may also drive variation in canopy  
84 complexity, irrespective of species diversity. Some savanna trees form denser canopies than  
85 others, as a result of variation in leaf size and branch architecture (Charles-Dominique et al.,  
86 2018). Previous studies have compared the branch architecture of ex-Acacia (e.g. *Senegalia* and  
87 *Vachellia* spp.) and miombo (e.g. *Julberardia*, *Brachystegia*, and *Isoberlinia*) archetypal tree  
88 species. While ex-Acacia species tend to inhabit drier, heavily grazed areas, miombo species tend  
89 to inhabit dystrophic wetter areas structured heavily by fire (Ribeiro et al., 2020). These studies  
90 have shown that ex-Acacia species develop sparser canopies, cagey branch architecture, and wider  
91 spreading crowns, while dominant Fabaceae species from the miombo develop thicker, taller

92 canopies, and can grow to larger sizes (Archibald & Bond, 2003; Mugasha et al., 2013; Privette  
93 et al., 2004). Similarly, dominant miombo Fabaceae species from the Detarioideae subfamily  
94 have been shown to develop wider crowns and grow taller than coexisting miombo species from  
95 the Combretaceae family. Shenkin et al. (2020) showed that Fabaceae tree species from tropical  
96 forests develop wider and more voluminous tree crowns than other common families of tropical  
97 trees. Under identical stem densities, miombo woodland species may therefore exclude grass  
98 more effectively than ex-Acacia or Combretaceae species given these differences in growth form.

99 Canopy complexity is multi-dimensional and has previously been explained using a plethora  
100 of simple metrics that originated in forest and community ecology (Kershaw et al., 2017).  
101 Assessments of canopy complexity have most often modelled tree canopies as a series of ellipses  
102 (2D), ellipsoids or cones (3D) based on field measurements with measuring tapes (Jucker et al.,  
103 2015). Measurements of this kind are time consuming and yet remain an over-simplification of  
104 canopy structure. Alternatively, canopy closure is often measured using indirect optical methods  
105 which partition sky from canopy material, i.e. with hemispherical photography or the commonly  
106 used LAI-2000, providing a 2D representation of the canopy but lacking information on vertical  
107 canopy structure (Jonckheere et al., 2004). In recent years, particularly in temperate and boreal  
108 forests, LiDAR (Light Detection And Ranging) has emerged as a suitable technology for rapidly  
109 and precisely assessing canopy structure in 3D, conserving information on 3D structure of the  
110 calibre that is required to understand it's complexities (Calders et al., 2020; Muir et al., 2018).  
111 In tropical savannas, very few studies have used terrestrial LiDAR for vegetation analyses, and  
112 in southern Africa all existing studies have been located at the Skukuza Flux Tower in Kruger  
113 National Park, South Africa (Muumbe et al., 2021). Pioneering work describing the ecology of  
114 southern African savannas placed large emphasis on canopy structural diversity as a mediator of  
115 ecosystem function (Solbrig et al., 1996), but much of that understanding of savanna vegetation  
116 structure was derived from traditional mensuration methods. Using terrestrial LiDAR to measure  
117 canopy complexity in southern African savannas therefore offers a unique chance to validate  
118 accepted theory and to describe differences in canopy structure among savanna vegetation types  
119 in finer detail than previously possible.

120 In this study I applied terrestrial LiDAR techniques to woodland-savanna mosaics at two sites in  
121 southern Africa, with the aim of increasing understanding of how various measures of tree canopy  
122 complexity relate to tree diversity and stand structure. I hypothesise that tree neighbourhoods  
123 with greater tree species diversity, greater heterogeneity in stem size, and greater heterogeneity in  
124 stem location, allow greater canopy complexity and foliage density. Thus, more diverse savannas  
125 might exhibit a higher potential woody biomass, greater productivity, and more effectively  
126 increase their growth under elevated atmospheric CO<sub>2</sub>, promoting woody thickening. I also  
127 consider the functional differences in canopy architecture among tree communities and how this  
128 affects canopy closure and total canopy occupancy.

## 129 2 Materials and methods

### 130 2.1 Study sites

131 Field measurements were conducted at two sites, Bicuar National Park, in southwest Angola  
132 (S15.1°, E14.8°), and Mtarure Forest Reserve, in southeast Tanzania (S9.0°, E39.0°) (Figure 1).  
133 At each site, 1 ha (100×100 m) plots were located in areas of savanna-woodland vegetation,  
134 across a gradient of stem density and covering a range of savanna floristic archetypes. In Angola,  
135 15 plots were sampled, while in Tanzania only seven were sampled following the curtailment of  
136 fieldwork due to COVID-19 travel restrictions. Fieldwork was conducted between February and  
137 April at both sites, during the peak growth period of each site in order to capture the maximum  
138 foliage volume in the canopy.

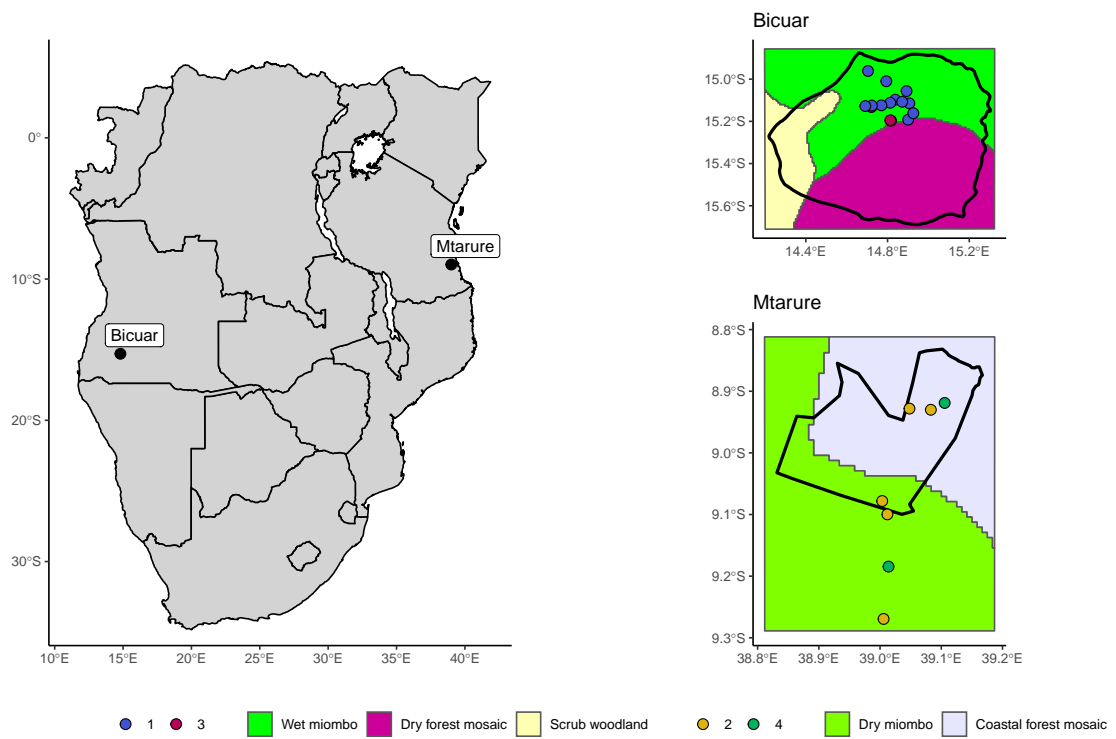


Figure 1: Location of study sites within southern Africa (left), and of 1 ha plots within each site (right). The black outlines in each site map denote the boundaries of protected areas which encompass the majority of study sites, Bicuar National Park in Angola (top), and Mtarure Forest Reserve in Tanzania (bottom). The background of each site map is a re-classified version of White's vegetation map (White, 1983). Points in site maps are shaded according to vegetation type identified by hierarchical clustering of tree genera abundances. Note that all maps are on different scales.

139 **2.2 Field measurements**

140 Within each 1 ha plot, each woody stem  $\geq 5$  cm stem diameter was identified to species, the  
141 stem Diameter at Breast Height (DBH) was measured at 1.3 m above the ground, and the stem  
142 location within the plot was recorded using tape measures. Each 1 ha plot was sampled by nine  
143 10 m diameter circular subplots arranged in a regular grid, with a 15 m buffer from the plot edge  
144 and 35 m between subplots. For each subplot, the distance and direction from the subplot centre  
145 of each stem  $> 5$  cm diameter with canopy material inside the subplot was recorded. Within each  
146 subplot, a variable number of scans were recorded using a Leica HDS6100 phase-shift Terrestrial  
147 Laser Scanner (TLS). The number and position of scans within a subplot was determined by  
148 the arrangement of canopy material in the subplot, to minimise shadows within the canopy of  
149 the subplot, and to maximise canopy penetration (Béland & Kobayashi, 2021). The number of  
150 scans per subplot ranged between one and five across both sites. Extended field methods and  
151 data analysis methods are described in Chapter 6.

152 **2.3 Data analysis**

153 **2.3.1 TLS processing**

154 Point clouds from scans in each subplot were registered and unified using Leica Cyclone (version  
155 9.1), with five reflective cross targets visible to all scans used as anchor points. Point clouds were  
156 voxelised to cubic voxels of different sizes depending on the application of the data. Subplot  
157 height profiles and canopy closure estimates were calculated using  $5 \text{ cm}^3$  voxels, while whole plot  
158 canopy rugosity and canopy surface roughness were calculated using  $50 \text{ cm}^3$  voxels. Voxels were  
159 classified as ‘filled’ if they intersected one or more points. Variation in voxel size reflects the  
160 spatial scale of each analysis, and is bounded by the beam divergence of the scanner over longer  
161 distances (Cifuentes et al., 2014). Choosing voxels that are too small can result in pock-marked  
162 representations of surfaces that are especially problematic when calculating larger scale canopy  
163 complexity metrics such as canopy top roughness, while voxels that are too large can result in  
164 an over-estimation of plant volume when estimating canopy foliage density at the subplot scale  
165 (Cifuentes et al., 2014; Seidel et al., 2012).

166 The noise reduction algorithm from Rusu et al. (2008) was used to discard points based on mean  
167 nearest neighbour distances, with a number of neighbours of eight, and a standard deviation  
168 threshold of 1.96. This effectively removed ‘ghost points’ produced by partial beam interceptions  
169 and also removed many erroneous returns caused by airborne dust particles, which was common  
170 at these study sites. Raw points clouds for each subplot had a mean of  $\sim 2.9 \times 10^8$  points,  $\sim 4.5 \times 10^7$   
171 points after voxelisation to  $5 \text{ cm}^3$ , and  $\sim 2.1 \times 10^7$  points after noise reduction.

172 Ground points were classified using the Progressive Morphological Filter (PMF) from Zhang  
173 et al. (2003). Point cloud height was reclassified based on this revised ground layer by measuring  
174 the vertical distance between the nearest ground point and each point. Points below 1.3 m  
175 height above ground were discarded for calculations of foliage density, canopy cover, and canopy  
176 complexity, as points below this threshold were often occupied by long grass.

177 **2.3.2 Canopy complexity metrics**

178 Ray-tracing was used to estimate canopy closure in each subplot, i.e. the proportion of the  
179 sky hemisphere occluded by plant material at the subplot centre from multiple TLS scans.  
180 Hemispherical images were created using the POV-Ray ray-tracing software (Persistence of  
181 Vision Pty. Ltd., 2004). Filled voxels were represented as black cubes filling the voxel volume,  
182 with a white sky box and no light source. A ‘camera’ with a  $180^\circ$  fisheye lens was placed at the

183 subplot centre within POV-Ray, at a height of 1.3 m pointing directly upwards. The images  
184 produced by POV-Ray were analysed using Hemiphot (ter Steege, 2018) to estimate canopy  
185 closure. Canopy closure estimates from the TLS were validated with hemispherical photographs  
186 taken at the same location and processed using the same method in Hemiphot, and compared  
187 using Pearson's correlation ( $r(195)=0.87$ ,  $p<0.001$ ). A plot level estimate of canopy closure was  
188 calculated as the mean of subplot canopy closure measurements. See Chapter 6 for expanded  
189 methods and explanation of the behaviour of the different canopy complexity metrics.

190 Effective Number of Layers (ENL) was calculated according to Ehbrecht et al. (2016) to measure  
191 vertical variation in subplot foliage density. ENL is calculated as the exponential Shannon index  
192 (i.e. the Hill number of order  $q = 1$ ) of foliage density among 50 cm vertical layers within each  
193 subplot:

$$\text{ENL} = \exp \left( - \sum_{i=1}^N p_i \times \ln p_i \right) \quad (1)$$

194 Where  $p_i$  is the proportion of filled voxels in the 50 cm layer  $i$ , and  $N$  is the total number  
195 of layers. ENL increases with canopy height and thus with number of layers, and also with  
196 variation in foliage density among those layers, but not with increased total foliage density.

197 Total foliage density was calculated within each subplot as the area under the curve of the foliage  
198 height profile. Total foliage density was also calculated at the plot level as the sum of filled 50  
199 cm<sup>3</sup> voxels across the plot. Vertical variation in subplot foliage density was calculated by fitting  
200 a linear model to the cumulative foliage density profile, then calculating the sum of squared  
201 residuals of that model.

202 Plot level canopy surface models were extracted using the 99th percentile of canopy height in 10  
203 cm<sup>2</sup> columns. A pit-filling algorithm provided by Khosravipour et al. (2014) was applied at 50  
204 cm<sup>2</sup> resolution to reduce the effects of incomplete canopy penetration in dense canopies. Whole  
205 plot canopy complexity was measured by three metrics. Canopy top roughness was measured  
206 as the coefficient of variation (CV) of canopy surface height across the plot. Canopy rugosity  
207 was measured according to Hardiman et al. (2011), as the CV of vertical and horizontal foliage  
208 density within 0.5 m<sup>3</sup> cubic bins. Finally, canopy height was calculated as the mean of the  
209 canopy surface roughness model across the plot.

### 210 2.3.3 Stand structure and diversity

211 An adapted version of the Iterative Hegyi index was used to estimate crowding at the subplot  
212 scale. The Iterative Hegyi Index was used as an alternative to stem density, which does not  
213 adequately capture crowding at small spatial scales when only a small number of trees are  
214 included in the sample (Hegyi, 1974). The CV of stem basal area was calculated as a measure of  
215 the heterogeneity of tree size in the subplot neighbourhood.

216 At the plot level, the regularity of species spatial distribution was estimated using the spatial  
217 mingling index (von Gadow & Hui, 2002), which scores each tree based on whether it shares  
218 species identity with its nearest neighbours. The spatial regularity of trees was estimated using  
219 the uniform angle index (winkelmaass) (von Gadow & Hui, 2002), which scores each tree based  
220 on the angles between nearest neighbours. Additionally, the degree of spatial clustering of trees  
221 was measured using Voronoi tessellation of tree locations., as the CV of Voronoi cell areas (Ong  
222 et al., 2012). Finally, plot level tree density was calculated to estimate crowding at the plot scale.  
223 See Chapter 6 for more information on the behaviour of the spatial mingling index, uniform  
224 angle index, and Voronoi cell area CV.

225 Species diversity at both the subplot and plot level was measured using the exponential Shannon

226 index (i.e. the Hill number of order  $q = 1$ ), calculated using tree species abundances (Jost,  
227 2006). At the subplot level trees were included if they had canopy material inside the 10 m  
228 diameter subplot, while at the plot level trees were included if the largest stem was inside the  
229 plot boundaries.

230 **2.3.4 Statistical analysis**

231 Non-metric Multi-dimensional Scaling (NMDS) was used to describe variation in species com-  
232 position among plots, using genus-level basal area weighted abundance in each plot. Stems that  
233 could not be identified to genus were excluded from this analysis, which accounted for 0.2%  
234 of the total basal area recorded. Four distinct vegetation types, two from each site (Table 1),  
235 were identified using hierarchical clustering of the four dominant NMDS ordination axes using  
236 Ward's algorithm. Clusters were further described using Dufrêne-Legendre indicator species  
237 analysis and by ranking tree species according to abundance across all plots within each cluster.

238 Linear mixed effects models tested the effects of tree species diversity and stand structural  
239 diversity on subplot canopy complexity metrics. Mixed models used a nested random intercept  
240 structure to account for the sampling design of subplots within plots and plots within vegetation  
241 types. Separate models were fitted for each canopy complexity metric, resulting in four models  
242 at the subplot level. Effect sizes among fixed effects in maximal models were compared for each  
243 canopy complexity metric, using the 95% confidence interval of the effect size to ascertain the  
244 significance of fixed effects by whether the confidence interval overlapped zero (Nakagawa &  
245 Cuthill, 2007). AIC values and Akaike weights of models with different combinations of fixed  
246 effects were compared to determine which combination of diversity and structural metrics best  
247 explained variation in each canopy complexity metric.

248 Statistical analysis of the determinants of plot level canopy complexity metrics were conducted  
249 using linear models. The ex-Acacia vegetation type was represented by only two plots and could  
250 not be included in this model due to lack of replication. As with the subplot linear mixed models,  
251 predictor variable effect sizes were used to assess predictor variable significance, and comparison  
252 of candidate models using AIC, Akaike weights, and model  $R^2$  values was used to determine  
253 which combination of predictors best explained each canopy complexity metric.

254 Path analysis was used to test whether tree species diversity influences canopy complexity  
255 indirectly through its effect on stand structure, using the `piecewiseSEM` R package (Lefcheck,  
256 2016). Two path analyses were conducted, one at the plot level and one at the subplot level.  
257 Subplot path analysis investigated the direct effect of species diversity on canopy closure, as  
258 well as the indirect effect of diversity on canopy closure via the CV of basal area, with random  
259 intercept terms for each vegetation type. Again, these models excluded the ex-Acacia vegetation  
260 type due to lack of replication. Plot level path analysis investigated the direct effects of species  
261 diversity and spatial mingling of species on mean canopy height, as well as the indirect effects of  
262 these metrics on canopy height via tree density and basal area CV. Again, ex-Acacia plots were  
263 excluded from this path analysis.

264 **3 Results**

265 **3.1 Description of vegetation types**

266 Indicator species analysis shows that the four vegetation types identified by hierarchical clustering  
267 constitute common southern African savanna floristic archetypes (Table 2). Cluster 1, found in  
268 Bicuar National Park contains typical miombo species from the Detarioideae subfamily, such  
269 as *Jubbernardia paniculata*. Cluster 1 is the most frequent vegetation type in this study, with

Table 1: Description of the vegetation type clusters, identified using Ward's algorithm based on basal area weighted genus abundance. AGB = Above-Ground woody Biomass. Species richness, stem density and AGB are reported as the median among plots, with the interquartile range in parentheses.

Site	Cluster	N sites	Richness	Stem density (stems ha <sup>-1</sup> )	AGB (t ha <sup>-1</sup> )
Bicuar	1	12	17(2)	642(194)	41( 8.4)
Mtarure	2	5	23(4)	411(137)	72(11.9)
Bicuar	3	3	6(1)	196( 55)	77( 7.3)
Mtarure	4	2	12(2)	288( 73)	9( 0.2)

Table 2: Floristic description of the vegetation type clusters. Dominant species are the most abundant individuals across all plots within each cluster. Indicator species are the three species with the highest indicator values, from Dufrêne-Legendre indicator species analysis.

Cluster	Dominant species	Indicator species	Indicator value
1	Julbernardia paniculata	Strychnos spinosa	0.83
	Burkea africana	Combretum collinum	0.74
	Combretum collinum	Julbernardia paniculata	0.70
2	Diplorhynchus condylocarpon	Pteleopsis myrtifolia	1.00
	Pseudolachnostylis maprouneifolia	Diplorhynchus condylocarpon	0.89
	Gymnosporia senegalensis	Pseudolachnostylis maprouneifolia	0.81
3	Baikiaea plurijuga	Baikiaea plurijuga	0.94
	Baphia massaiensis	Baphia massaiensis	0.83
	Philenoptera nelsii	Philenoptera nelsii	0.45
4	Combretum apiculatum	Vachellia nilotica	0.99
	Burkea africana	Combretum apiculatum	0.70
	Bauhinia petersiana	Senegalia polyacantha	0.62

270 12 plots. Cluster 1 has the highest stem density, but lower Above-Ground woody Biomass  
271 (AGB) than Clusters 2 or 3, which contain larger individuals with disproportionately higher  
272 biomass. Cluster 2, found in Mtarure Forest Reserve, is dominated by *Pteleopsis myrtifolia*,  
273 a common miombo species from the Combretaceae family. Indeed, Cluster 2 also contained  
274 other common miombo species shared with plots in Cluster 1, such as *Julbernardia globiflora*  
275 and *Pseudolachnostylis maprouneifolia*, but these clusters remain distinct due to biogeographic  
276 variation in endemic genera at the longitudinal extremes of the miombo ecoregion represented  
277 by the two sites in this study. Cluster 3 represents *Baikiaea* woodland, found on Kalahari sands  
278 in southern Angola. It is species poor and dominated by *Baikiaea plurijuga* which forms large  
279 spreading canopy trees with high AGB. Other shrubby species that coppice readily in response  
280 to disturbance by fire such as *Baphia massaiensis* are also common. Cluster 4, found in Mtarure  
281 is a type of ex-Acacia woodland, dominated by *Vachellia* and *Senegalia* spp. This vegetation  
282 type was not well represented in the study, with only two plots, precluding its use in some  
283 multi-level statistical analyses at the plot level due to lack of replication. Cluster 4 had far lower  
284 AGB than the other clusters (Table 1).

285 Differences in canopy structure among the four vegetation types are evident through observation  
286 of canopy surface models for typical plots within each vegetation type (Figure 5), and by  
287 comparing canopy complexity metrics (Figure 6). Cluster 1 shows many overlapping crowns  
288 forming a nearly contiguous canopy surface, and the highest plot foliage density of all clusters.  
289 Though the tallest trees in Cluster 1 have smaller crowns than those in Cluster 2, which also  
290 forms a nearly contiguous canopy. The largest trees in Cluster 2 grow taller and have a wider  
291 spreading canopy than those in other vegetation types. Cluster 3 shows two distinct size classes  
292 of tree, the large *Baikiaea plurijuga* forming clear isolated canopies, and much smaller scattered  
293 shrubby individuals in the understorey. Cluster 4 shows many small shrubby individuals with  
294 irregular canopy shapes, but a greater total crown area coverage than Cluster 3.

### 295 3.2 Bivariate relationships

296 Bivariate plots and linear models show that subplot species diversity, measured as the true-  
297 numbers equivalent of the Shannon diversity index of the tree neighbourhood around each 10 m  
298 diameter subplot, appears to have weak positive effects on subplot canopy layer diversity, canopy  
299 closure and foliage density (Figure 3, Table 3). The Hegyi crowding index had strong positive  
300 effects on canopy closure and layer diversity, as expected. The effect of Hegyi crowding on  
301 subplot canopy complexity metrics was similar across all vegetation types (Table 6). Structural  
302 diversity, measured as the CV of subplot stem basal area had significant weak positive effects on  
303 total canopy foliage, layer diversity, and canopy closure.

304 At the plot level, effects of species diversity and stand structure on canopy complexity were  
305 similarly weak, but not strictly significant except for the effect on canopy height, which explained  
306 more variance in canopy height than tree density (Figure 4, Table 3). The effect of spatial  
307 regularity of stems on canopy closure, measured by uniform angle index, was clearly negative,  
308 while the effect of spatial clustering of stems, measured by Voronoi cell area CV, was negligible.  
309 Additionally, there was a non-significant negative effect of basal area CV on whole canopy  
310 rugosity. As expected, tree density had strong positive and significant effects on foliage density  
311 and canopy closure, but negative effects on canopy roughness and canopy rugosity. Cluster 4  
312 represented an outlier in plot level bivariate relationships, with low canopy closure, low canopy  
313 height, low species diversity, and low variation in stem size.

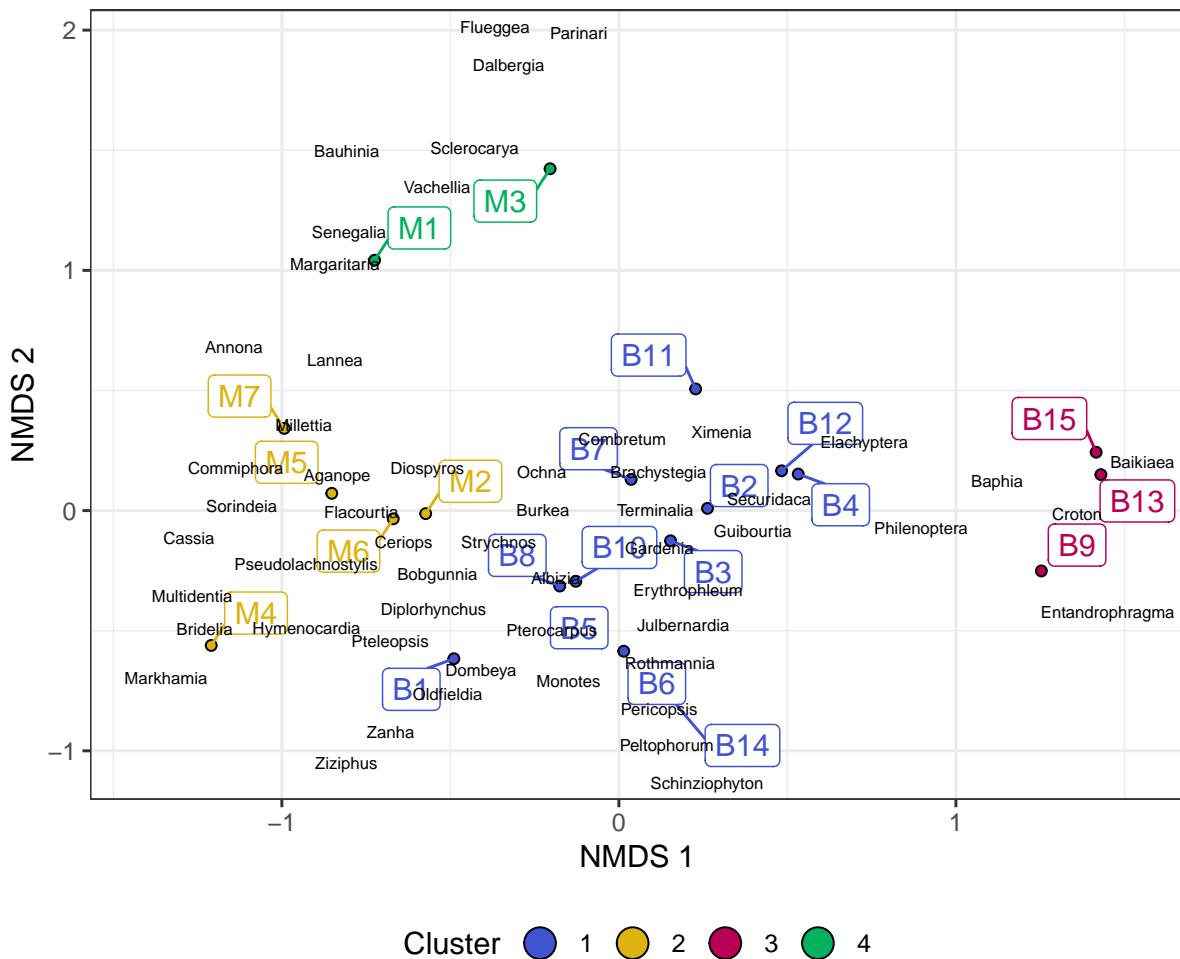


Figure 2: The first two axes of a Non-metric Multi-Dimensional Scaling (NMDS) analysis of tree genus diversity in each plot. Genus scores are labelled as black text, while plot scores are labelled as coloured points. Plots are shaded by vegetation type, identified by hierarchical clustering: 1) B1-B8, B10-B12, B14, dominated by core miombo species such as *Julbernardia* spp., *Brachystegia* spp.; 2) M2, M5, M6, and M7, also dominated by core miombo genera with some genera not found in Bicuar National Park such as *Commiphora* and *Sorindeia*; 3) B9, B13 and B15, dominated by *Baikiaea plurijuga*; and 4) M1, M3, and M4, dominated by *Senegalia* spp., *Vachellia* spp., and *Combretum* spp.

Table 3: Summary statistics of bivariate linear models comparing canopy complexity metrics with diversity and stand structural metrics across all vegetation types. Slope refers to the slope of the predictor term in the model,  $\pm 1$  standard error. T is the t-value of the slope of the predictor term in the model, Asterisks indicate the p-value of these terms ( $^{***}<0.001$ ,  $^{**}<0.01$ ,  $^{*}<0.05$ ).

Response	Predictor	Slope	F	R <sup>2</sup>	T
Foliage density	Basal area CV	8.7e+01 $\pm$ 3.0e+01	8.6(2,167)	0.05	2.93**
	Hegyi	7.8e+03 $\pm$ 1.6e+03	25.5(2,184)	0.12	5.05***
	Shannon	3.2e+03 $\pm$ 1.1e+03	8.9(2,180)	0.05	2.98**
Canopy closure	Basal area CV	1.2e-03 $\pm$ 4.8e-04	6.3(2,168)	0.04	2.52*
	Hegyi	2.4e-01 $\pm$ 2.1e-02	132.8(2,185)	0.42	11.52***
	Shannon	4.7e-02 $\pm$ 1.7e-02	7.3(2,181)	0.04	2.70**
Foliage uniformity	Basal area CV	4.1e+00 $\pm$ 3.0e+00	1.9(2,167)	0.01	1.37
	Hegyi	4.0e+02 $\pm$ 1.6e+02	6.2(2,184)	0.03	2.49*
	Shannon	2.2e+02 $\pm$ 1.1e+02	4.1(2,180)	0.02	2.04*
Layer diversity	Basal area CV	3.2e-02 $\pm$ 7.6e-03	17.6(2,167)	0.10	4.20***
	Hegyi	2.7e+00 $\pm$ 3.9e-01	46.8(2,184)	0.20	6.84***
	Shannon	1.1e+00 $\pm$ 2.7e-01	16.8(2,180)	0.09	4.10***
Canopy roughness	Basal area CV	3.0e-02 $\pm$ 5.0e-02	0.4(2,16)	0.02	0.60
	Voronoi CV	7.5e-01 $\pm$ 5.9e-01	1.6(2,16)	0.09	1.26
	Mingling	-2.8e+01 $\pm$ 3.3e+01	0.7(2,16)	0.04	-0.86
	Tree density	-2.6e-02 $\pm$ 1.7e-02	2.3(2,16)	0.12	-1.51
	Shannon	-1.9e+00 $\pm$ 9.5e-01	4.0(2,16)	0.20	-2.01
	Uniform angle index	1.6e+02 $\pm$ 1.6e+02	1.0(2,16)	0.06	0.98
Canopy height	Basal area CV	7.1e-03 $\pm$ 7.3e-03	0.9(2,16)	0.06	0.97
	Voronoi CV	-4.7e-02 $\pm$ 9.1e-02	0.3(2,16)	0.02	-0.52
	Mingling	3.8e+00 $\pm$ 4.8e+00	0.6(2,16)	0.04	0.79
	Tree density	4.3e-03 $\pm$ 2.5e-03	3.1(2,16)	0.16	1.76
	Shannon	3.3e-01 $\pm$ 1.3e-01	6.0(2,16)	0.27	2.45*
	Uniform angle index	-2.2e+01 $\pm$ 2.4e+01	0.8(2,16)	0.05	-0.90
Canopy closure	Basal area CV	8.5e-04 $\pm$ 5.7e-04	2.2(2,20)	0.10	1.50
	Voronoi CV	2.4e-03 $\pm$ 5.8e-03	0.2(2,20)	0.01	0.41
	Mingling	7.2e-03 $\pm$ 3.7e-01	0.0(2,20)	0.00	0.02
	Tree density	4.7e-04 $\pm$ 1.9e-04	6.3(2,20)	0.24	2.50*
	Shannon	1.0e-02 $\pm$ 1.2e-02	0.7(2,20)	0.04	0.86
	Uniform angle index	-3.4e+00 $\pm$ 1.7e+00	3.9(2,20)	0.16	-1.98
Foliage density	Basal area CV	5.8e+01 $\pm$ 3.2e+01	3.3(2,16)	0.17	1.80
	Voronoi CV	5.8e+02 $\pm$ 4.1e+02	2.1(2,16)	0.11	1.43
	Mingling	6.6e+03 $\pm$ 2.3e+04	0.1(2,16)	0.01	0.29
	Tree density	3.0e+01 $\pm$ 1.0e+01	8.6(2,16)	0.35	2.93**
	Shannon	1.1e+03 $\pm$ 6.9e+02	2.5(2,16)	0.13	1.57
	Uniform angle index	-2.1e+04 $\pm$ 1.1e+05	0.0(2,16)	0.00	-0.18
Canopy rugosity	Basal area CV	-1.0e+00 $\pm$ 5.3e-01	3.7(2,16)	0.19	-1.92
	Voronoi CV	-6.0e+00 $\pm$ 7.0e+00	0.7(2,16)	0.04	-0.86
	Mingling	1.3e+02 $\pm$ 3.8e+02	0.1(2,16)	0.01	0.33
	Tree density	-5.2e-01 $\pm$ 1.7e-01	10.0(2,16)	0.38	-3.16**
	Shannon	-1.3e+01 $\pm$ 1.2e+01	1.2(2,16)	0.07	-1.11
	Uniform angle index	-1.8e+03 $\pm$ 1.9e+03	0.9(2,16)	0.06	-0.97

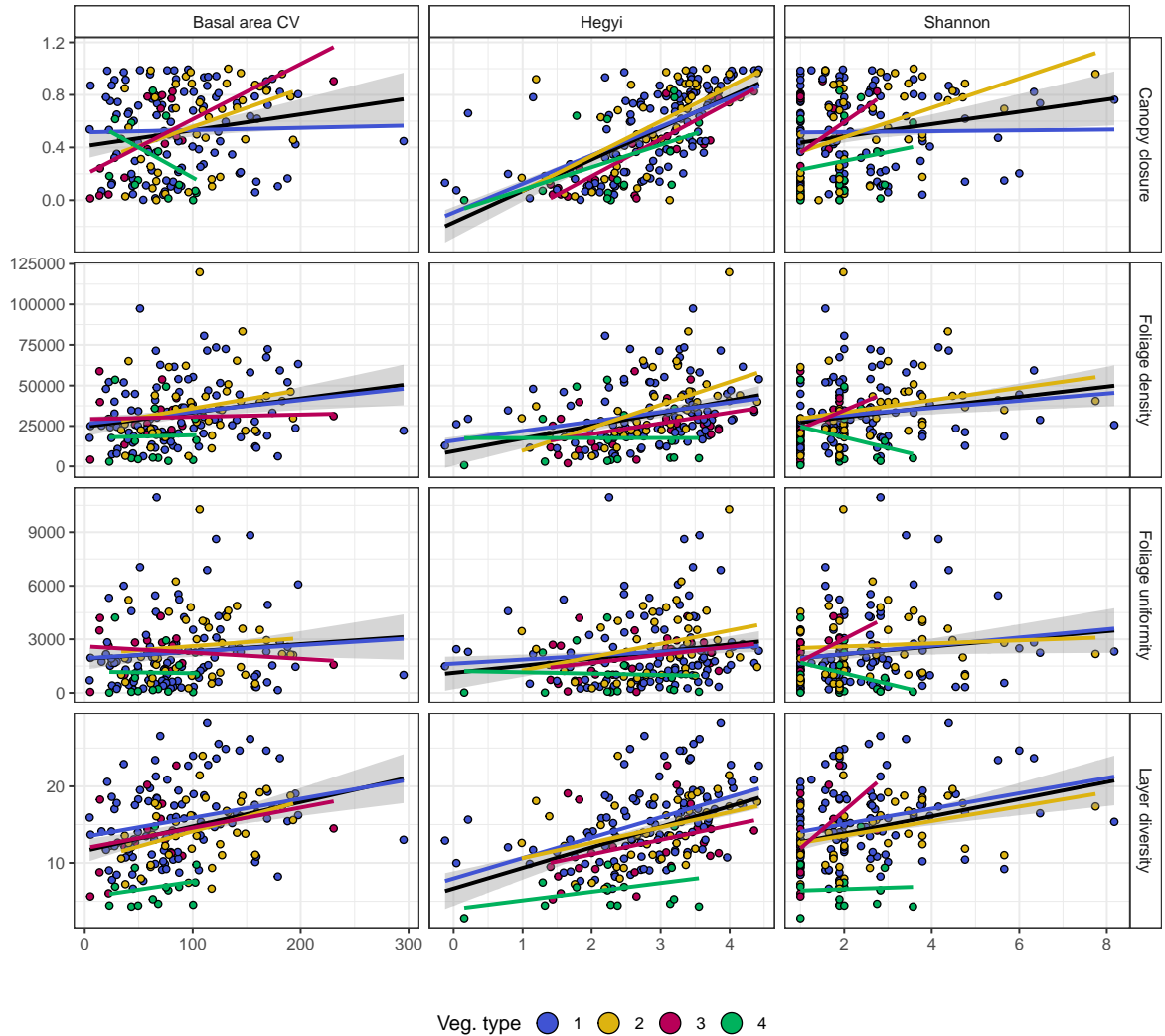


Figure 3: Subplot level bivariate relationships between diversity/stand structure metrics (x axis) and canopy complexity metrics (y axis). Points and linear model lines of best fit are coloured by vegetation type. Black lines of best fit are linear models including all plots, with a 95% confidence interval. See Table 6 for a comparison of linear model fits by vegetation type.

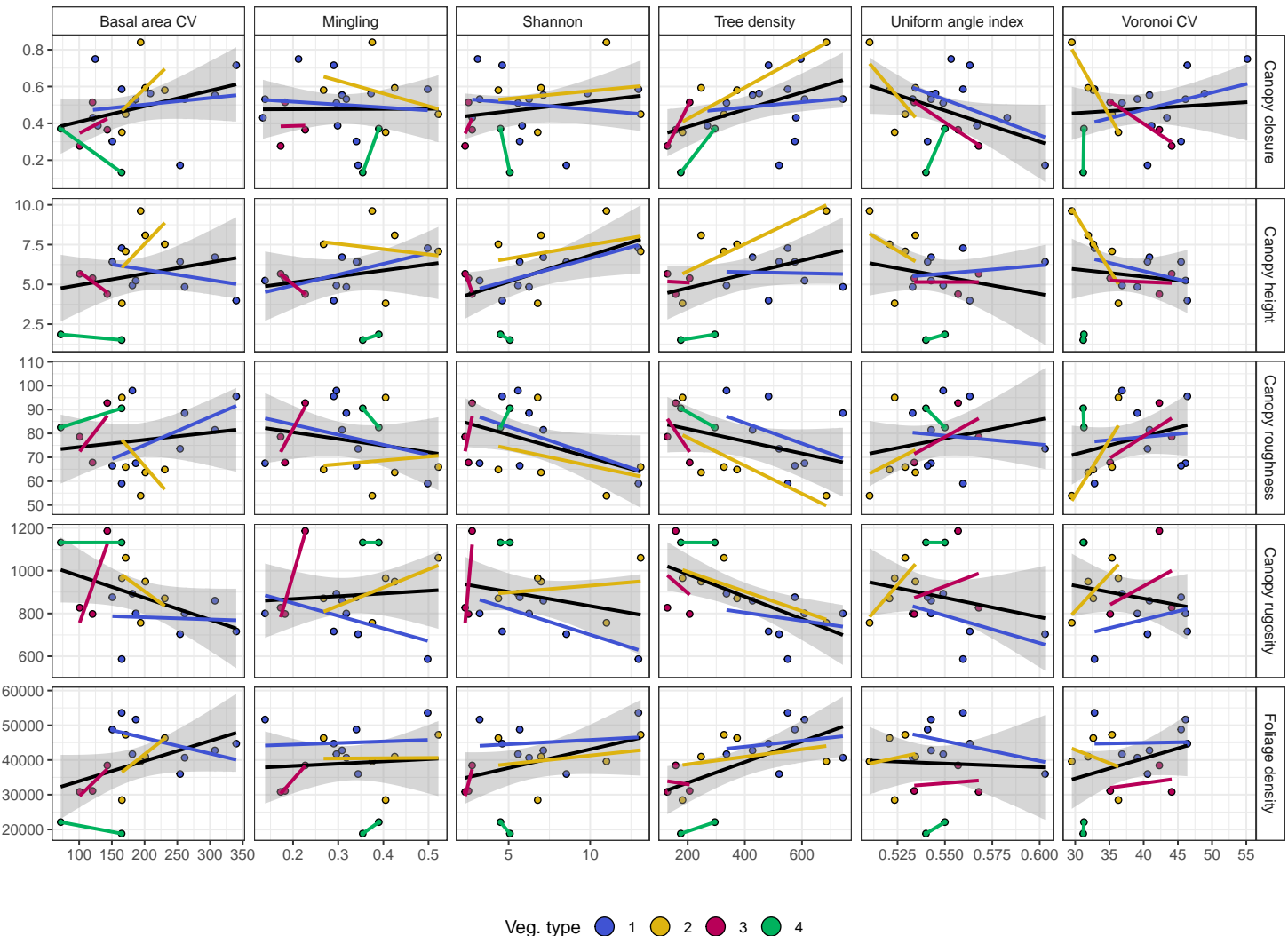


Figure 4: Plot level bivariate relationships between diversity/stand structure metrics (x axis) and canopy complexity metrics (y axis). Points and linear model lines of best fit are coloured by vegetation type. Black lines of best fit are linear models including all plots, with a 95% confidence interval. See Table 6 for a comparison of linear model fits by vegetation type.

Table 4: Explanatory variables included in the best model for each subplot canopy complexity variable.  $\Delta\text{AIC}$  shows the difference in model AIC value compared to a null model which included only the random effects of vegetation type and plot.  $\Delta\text{AIC}$  values  $>2$  indicate that the model is of better quality than the null model.  $R^2_c$  is the  $R^2$  of the best model, while  $R^2_m$  is the  $R^2$  of the model fixed effects only.

Response	Hegyi	Shannon	Basal area CV	$\Delta\text{AIC}$	$R^2_c$	$R^2_m$
Layer diversity	✓	✓	✓	37.0	0.50	0.17
Foliage density	✓		✓	47.6	0.27	0.09
Foliage uniformity	✓			13.1	0.28	0.02
Canopy closure	✓	✓		101.9	0.60	0.46

### 314 3.3 Subplot mixed models

315 Linear mixed effects models showed that species diversity of the subplot neighbourhood con-  
 316 tributed to both layer diversity and canopy closure (Table 4), despite their low  $R^2$  in bivariate  
 317 linear models, and low effect sizes in maximal linear mixed models (Figure 7). As also seen in  
 318 the subplot bivariate relationships Figure 3, the Hegyi crowding index had strong positive effects  
 319 on canopy closure and layer diversity, though these effects were non-significant for vegetation  
 320 Clusters 3 and 4. Stem basal area CV had a significant positive effect on layer diversity and  
 321 foliage density, but there was wide variation in vegetation type marginal effects for Clusters 3  
 322 and 4, due to low levels of replication. Cluster 3 had strong positive effects of species diversity  
 323 on foliage uniformity and layer diversity. The random effects of vegetation type and plot identity  
 324 described most of the variation in layer diversity and foliage density. Foliage uniformity was  
 325 poorly explained by all combinations of fixed effects, with the best model only explaining 29%.  
 326 All models were better than random effects only models according to AIC values (Table 4).

### 327 3.4 Plot level linear models

328 While species diversity had varying effects on different plot level canopy complexity metrics, the  
 329 confidence intervals on these effect sizes were wide (Figure 8). Species diversity had a significant  
 330 positive effect on canopy height ( $\beta=3\pm0.96$ ,  $p<0.05$ ), a non-significant positive effect on canopy  
 331 closure ( $\beta=0.07\pm0.085$ ,  $p=0.41$ ), but a negative effect on canopy surface roughness ( $\beta=-13\pm6.8$ ,  
 332  $p=0.09$ ) and whole canopy rugosity ( $\beta=-111\pm71$ ,  $p=0.15$ ). Spatial mingling of tree species had a  
 333 positive effect on canopy surface roughness and canopy rugosity, but a negative effect on canopy  
 334 height. Plot tree density had negligible effects on canopy complexity, except for canopy rugosity  
 335 ( $\beta=-61\pm42$ ,  $p=0.17$ ), in contrast to the effect of Hegyi crowding on subplot canopy complexity.  
 336 Measures of structural diversity, measured by the uniform angle index, Voronoi cell area CV,  
 337 and basal area CV, had smaller effects on canopy complexity than species diversity, and were  
 338 generally insignificant. One exception was the effect of uniform angle index, i.e. the spatial  
 339 clustering of stems, on canopy closure, which was clearly negative, though still insignificant  
 340 ( $\beta=-0.08\pm0.043$ ,  $p=0.1$ ), the effect of Voronoi cell area CV on foliage density, which was positive  
 341 ( $\beta=6199\pm3312$ ,  $p=0.09$ ), and the effect of basal area CV on canopy closure, which was positive  
 342 ( $\beta=0.06\pm0.042$ ,  $p=0.19$ ).

343 Despite the weak effect sizes of species diversity on canopy complexity at the plot level, model  
 344 selection showed that foliage density, canopy height and canopy roughness were better explained  
 345 by models which included species diversity (Table 5). Additionally, the best models for canopy  
 346 height and canopy roughness also included spatial mingling of tree species. The model for canopy

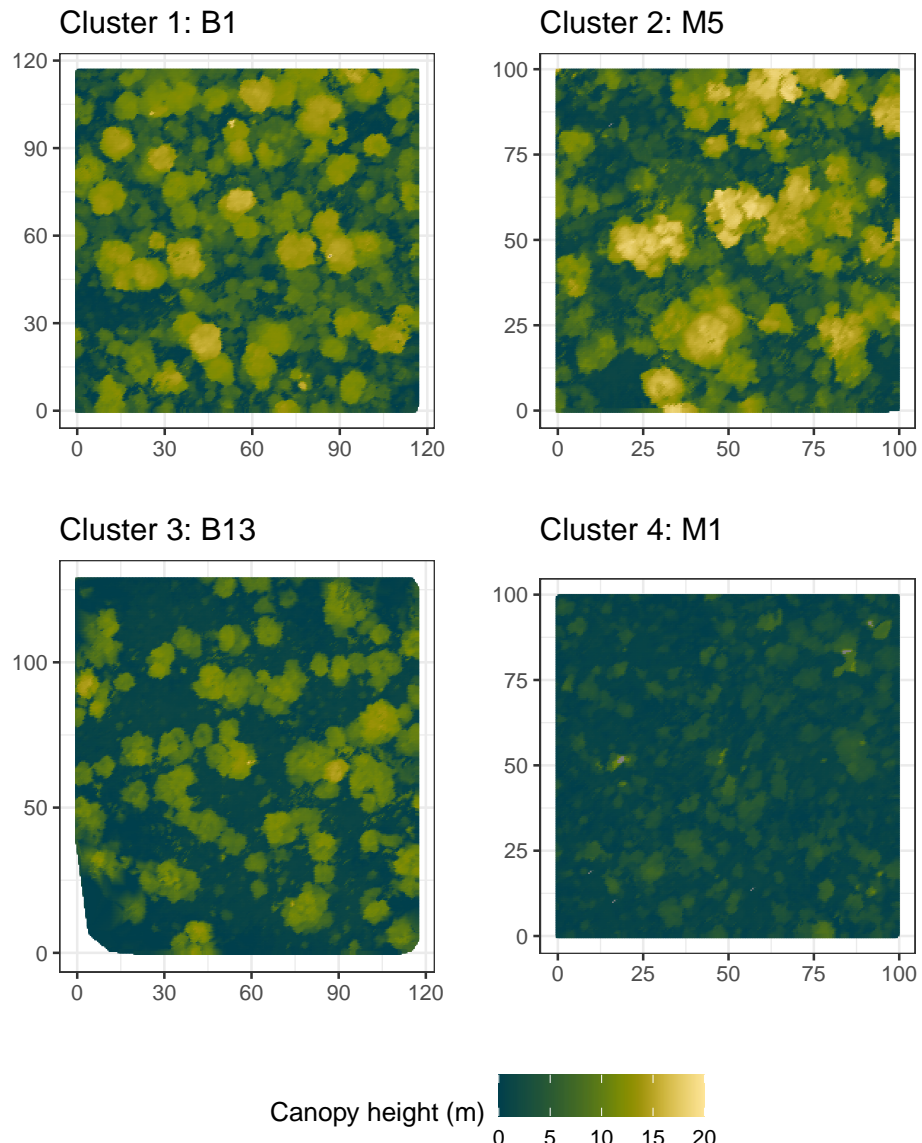


Figure 5: Representative canopy surface models for each vegetation type identified in the hierarchical clustering analysis. Panel titles show the plot name and the vegetation type cluster.

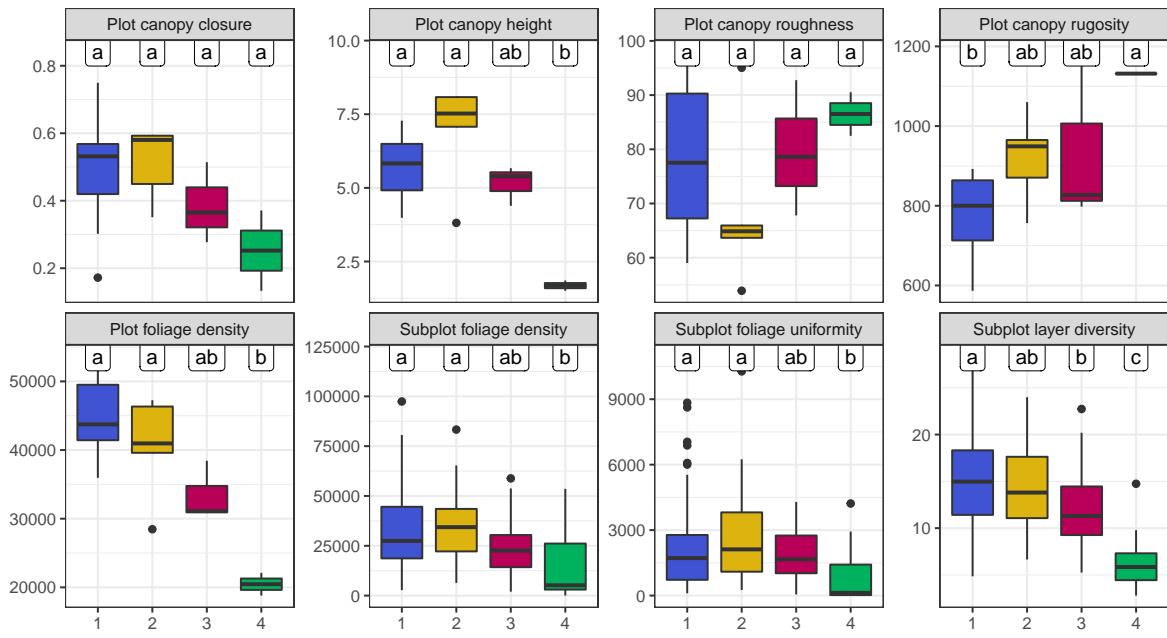


Figure 6: Box plots showing variation in canopy complexity metrics among the four vegetation types identified in the hierarchical clustering analysis. Thick lines show the median, boxes show the interquartile range (IQR), whiskers show  $1.5 \times \text{IQR}$ , and points show outliers beyond these limits. Labels above each box plot group vegetation types according to significant differences in pairwise Tukey's tests; vegetation types sharing a letter are not significantly different.

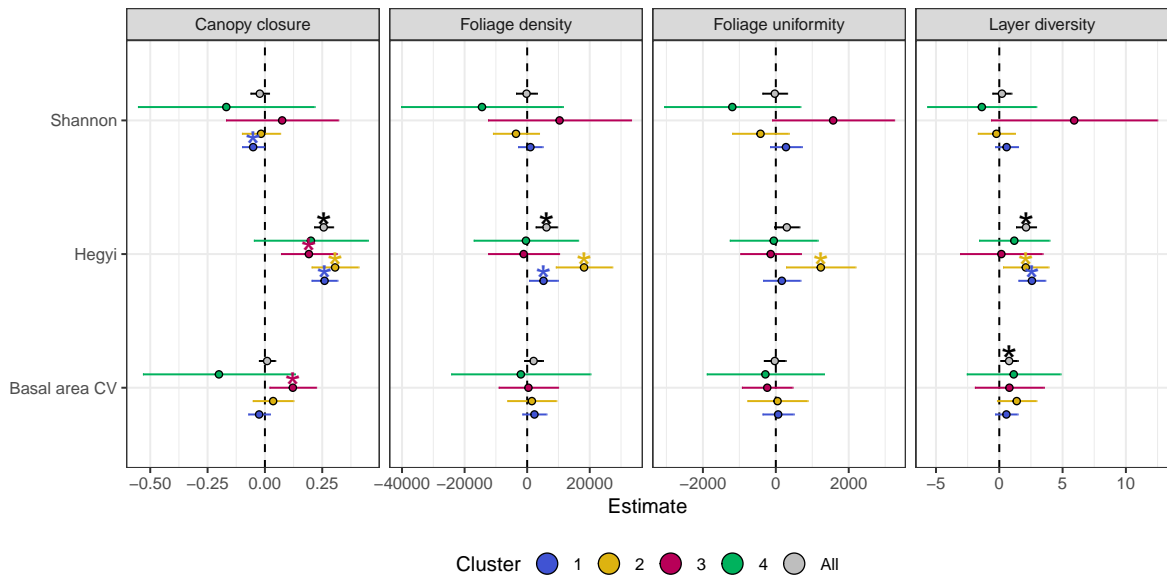


Figure 7: Standardised fixed effect slopes for each subplot canopy complexity metric model metric. Slope estimates where the interval ( $\pm 1$  standard error) does not overlap zero are considered to be significant effects, marked with asterisks. Points are coloured according to vegetation type.

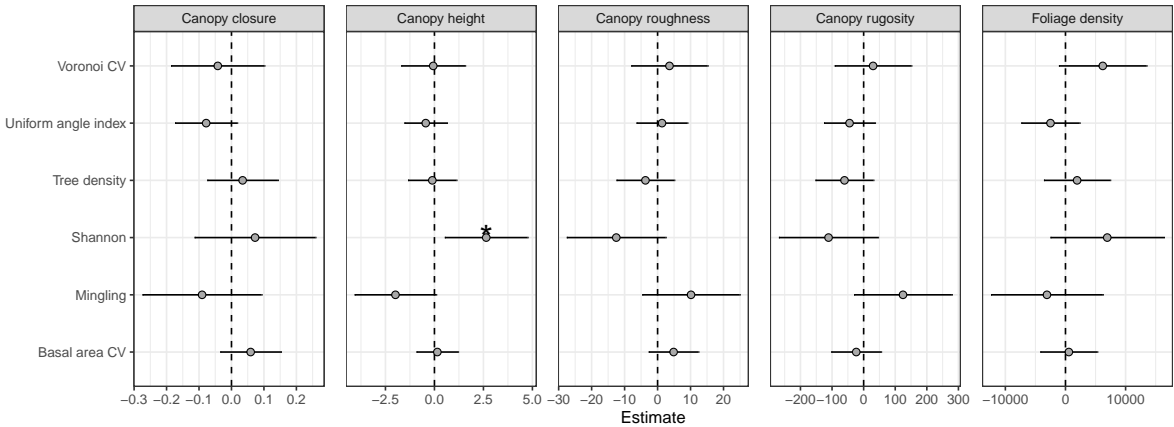


Figure 8: Standardised effect sizes for whole-plot canopy rugosity. Slope estimates where the interval ( $\pm 1$  standard error) does not overlap zero are considered to be significant effects, marked with asterisks.

Table 5: Explanatory variables included in the best linear model for each plot-level canopy complexity metric.  $\Delta\text{AIC}$  shows the difference in model AIC value compared to a null model.  $\Delta\text{AIC}$  values  $> 2$  indicate that the model is of better quality than the null model.

Response	Shannon	Tree density	Basal area CV	Mingling	Uniform angle index	Voronoi CV	$\Delta\text{AIC}$	$R^2$	Prob.
Foliage density	✓					✓	5.8	0.42	$<0.05$
Canopy closure			✓			✓	5.8	0.42	$<0.05$
Canopy height	✓			✓			8.2	0.49	$<0.01$
Canopy roughness	✓				✓		2.5	0.30	0.07
Canopy rugosity		✓				✓	6.9	0.45	$<0.05$

347 roughness was only marginally better than a null model and the model did not have a significant  
 348 p-value.

### 349 3.5 Path analysis

350 The subplot level path analysis investigating the indirect effect of subplot species diversity on  
 351 canopy closure via the basal area CV showed that while species diversity had a strong positive  
 352 significant effect on basal area variation, the effect of basal area variation on canopy closure  
 353 remained negligible (Figure 9). The indirect effect of species diversity on canopy closure via  
 354 basal area CV was -0.0016, while the direct effect was 0.078. The  $R^2$  of this model was 0.47. As  
 355 in the bivariate relationships and plot level linear models, species diversity had a weak positive  
 356 significant effect on canopy closure, while the major driver of canopy closure was the Hegyi  
 357 crowding index.

358 The plot level path analysis, which tested the effects of species diversity and species mingling  
 359 on canopy height, showed that the main effect of species diversity on canopy height was direct  
 360 (1.3\*), while the indirect effects via basal area CV (0.0210), and tree density (-0.0294), remained  
 361 small and insignificant. Shannon diversity had a strong positive effect on tree density. Species  
 362 mingling had a moderately strong negative but insignificant direct effect on canopy height, as in  
 363 the linear mixed models and bivariate relationships.

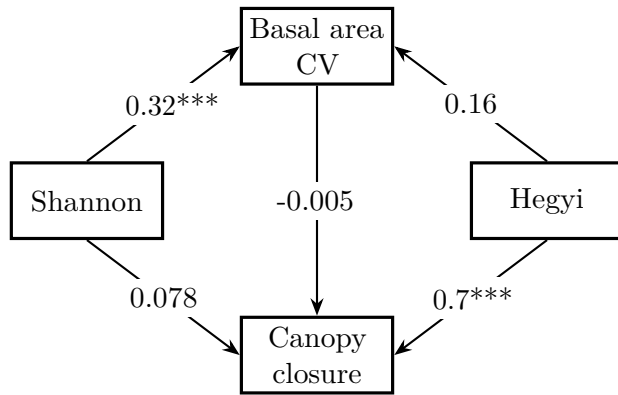


Figure 9: Directed Acyclic Graph showing standardised path coefficients of paths in the path analysis of the indirect effect of subplot species diversity (Shannon diversity index) on canopy closure via basal area CV. Asterisks define p-value thresholds: \* $<0.05$ , \*\* $<0.01$ , \*\*\* $<0.001$ .

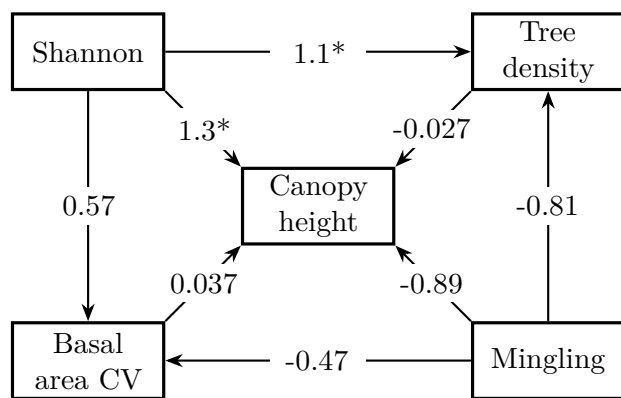


Figure 10: Directed Acyclic Graph showing standardised path coefficients of paths in the path analysis of the indirect effect of plot species diversity (Shannon diversity index) and species mingling on mean canopy height via stand structural metrics of basal area CV and tree density. Asterisks define p-value thresholds: \* $<0.05$ , \*\* $<0.01$ , \*\*\* $<0.001$ .

364 **3.6 Covariance of subplot and plot measures of canopy complexity**

365 Plot and subplot canopy complexity metrics were highly correlated in many cases, with similar  
366 relationships among vegetation types (Figure 8, Figure 12, Figure 13). Most subplot and plot  
367 level canopy metrics covaried in a predictable manner. For example, increased canopy height  
368 led to an increase in canopy closure. Plot canopy height especially, tended to be strongly  
369 positively correlated with subplot canopy complexity metrics. Additionally, as canopy rugosity  
370 increased, many subplot canopy complexity and density metrics decreased. Subplot metrics  
371 varied greatly within plots, producing large uncertainty in plot level estimates of these metrics.  
372 All subplot level canopy complexity metrics positive correlated with each other (Figure 13). Plot  
373 level canopy complexity also generally correlated (Figure 12). Plot level measures of spatial  
374 heterogeneity in canopy structure, i.e. canopy surface roughness and canopy rugosity, were  
375 negatively correlated with measures of canopy density, i.e. foliage density, canopy closure, and  
376 canopy height. Measures of canopy spatial heterogeneity positively correlated with each other,  
377 as did measures of canopy density.

378 **4 Discussion**

379 This study investigated relationships between tree species diversity, stand structure, and several  
380 metrics of tree canopy complexity using terrestrial LiDAR in southern African savannas, with a  
381 view to improving understanding of the biotic drivers of variation in canopy complexity and  
382 vegetation dynamics. Species diversity appeared to generally have weak positive effects on canopy  
383 complexity metrics related to canopy density at both the subplot and plot scales. Plots with  
384 greater species diversity produced taller tree canopies, with greater canopy closure and foliage  
385 density. Species diversity had negative effects on canopy surface roughness and canopy rugosity,  
386 canopy complexity metrics both related to the spatial heterogeneity of foliage distribution. The  
387 study did not however, find support for the hypothesis that increased heterogeneity in tree stem  
388 size causes an increase in canopy complexity, and only partial support for the hypothesis that  
389 greater heterogeneity in stem location causes increased canopy complexity. This study supports  
390 previous studies in forests which found a positive association between tree species diversity and  
391 canopy space-filling (Seidel et al., 2013; Shirima et al., 2015).

392 **4.1 Ecological consequences of a species diversity effect on canopy complexity**

393 The result that species diversity increases metrics of canopy density suggests that diverse stands  
394 can more effectively close the tree canopy under a given set of environmental conditions. Of  
395 course, environmental conditions remain the largest determinant of canopy cover and were not  
396 measured here. There are climate thresholds which may prevent canopy closure even in diverse  
397 savannas (Devine et al., 2017). Increased canopy closure reduces light penetration to the ground  
398 (Pilon et al., 2020), reducing grassy fuel load, and so could promote woody densification in  
399 diverse stands under atmospheric CO<sub>2</sub> enrichment. Similarly, the finding that species diversity  
400 causes an increase in foliage density and canopy height suggests that more diverse stands  
401 could more effectively upregulate productivity in response to atmospheric CO<sub>2</sub> fertilisation, and  
402 can maintain stands with greater woody biomass. Taller trees hold disproportionately higher  
403 biomass than shorter trees (King, 1990). In mesic savannas that are prone to disturbance by  
404 fire, increased growth rate and canopy height could increase the likelihood of trees escaping  
405 the “fire trap”, and facilitate their growth to larger canopy trees (Wakeling et al., 2011). This  
406 finding concurs with many previous studies, which have found that species diversity leads to  
407 greater woody productivity in both forests and savannas (Liang et al., 2016; Plas, 2019). This  
408 study adds further information on the mechanisms underlying the species diversity effect on

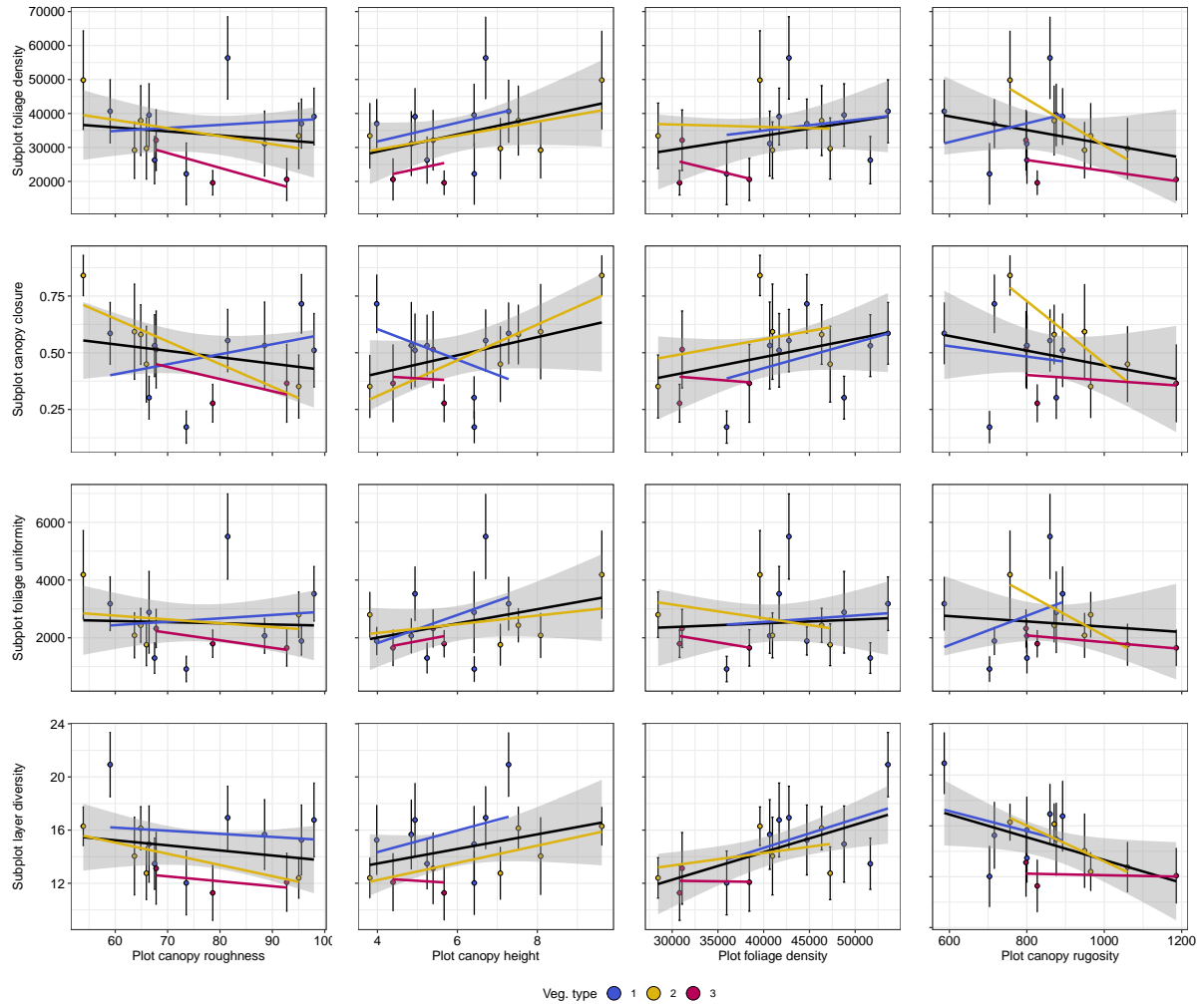


Figure 11: Bivariate plots comparing canopy structural metrics at the plot (x axis) and subplot scale (y axis). Each point represents the mean values of a single plot. Points and linear model fits are coloured according to vegetation type. The black linear model combines all vegetation types. Error bars on points are the standard deviation of mean subplot metrics across the plot. Note that because plot level canopy closure is calculated as the mean of subplot canopy closure, a comparison of subplot and plot canopy closure is not made in this figure.

409 ecosystem function in savannas, that niche complementarity among species promotes greater  
410 canopy occupancy.

## 411 **4.2 Species diversity and variation in tree size**

412 Path analysis showed that indirect effects of species diversity on canopy complexity via tree  
413 stem size (basal area CV) were negligible, due to the lack of an effect of tree stem size on canopy  
414 complexity at both the subplot and plot scale. This finding suggests that the effects of species  
415 diversity on canopy complexity are not simply due to covariation with heterogeneity of tree  
416 stem size, which could also arise due to demographic effects, rather they are due to differences  
417 among species in their canopy dimensions and growth strategy. This strengthens support for the  
418 hypothesis that species diversity genuinely increases canopy complexity, and is not merely an  
419 artefactual relationship arising from covariation. Previous studies in temperate and boreal forests  
420 have suggested that increasing tree stem size diversity through active management and thinning  
421 can offset productivity losses caused by reduced species diversity (Levick et al., 2009), but this  
422 study suggests that in southern African savannas at least, this is not the case. Furthermore, the  
423 lack of a strong effect of tree size variation on canopy complexity suggests a partial decoupling of  
424 tree size and foliage volume, and highlights species-specific differences in the plasticity of crown  
425 shape, and physiological limits on crown architecture that lead to species diversity effects on  
426 canopy packing separate from differences in tree size.

427 Shannon diversity did have strong positive effects on tree stem size variation and tree density.  
428 This can be interpreted as a niche complementarity effect, where diverse savannas are able  
429 to support a greater density of trees by reducing the effects of intraspecific competition and  
430 promoting canopy occupation in different vertical layers by trees of different sizes. Although  
431 basal area CV was included in best models for subplot layer diversity and foliage density, subplot  
432 level path analysis suggests that covariance between basal area CV and species diversity, and  
433 the strong direct effect of species diversity on canopy complexity, means that any observed effect  
434 of basal area CV on subplot canopy complexity is actually due to species diversity rather than  
435 covarying with basal area CV.

436 Despite tree density having strong positive observed effects on canopy density, and negative  
437 effects on canopy heterogeneity metrics in bivariate relationships, tree density only appeared  
438 in the best quality plot level mixed model for canopy rugosity. Additionally, the effect sizes  
439 for tree density in maximal mixed models were small. At the subplot level however, the Hegyi  
440 crowding index, which can be seen as analogous to tree density at neighbourhood scales, was a  
441 strong determinant of canopy complexity. Tree density was shown to covary with basal area CV  
442 and Voronoi cell area CV at the plot scale, which described variation in tree size and degree  
443 of spatial clustering, respectively. This covariance may have led to the effect dropping out in  
444 the best models at the plot scale, while at the subplot scale there were no measures of spatial  
445 clustering included. Hegyi crowding and tree density are expected to positively correlate with  
446 resource availability, and negatively correlate with disturbance which causes tree mortality and  
447 reduces tree growth. The study sites sampled here did cover a gradient of tree density, but  
448 variation in tree density within vegetation types was small. As vegetation type was included as  
449 a random effect in mixed models, this may have led to tree density not having a larger effect  
450 size in the models.

451 Variation in tree size caused positive canopy complexity effects for within-canopy structural  
452 metrics such as layer diversity and canopy surface roughness, but had negligible effects on canopy  
453 density. This is in line with other studies in forest ecosystems, which report that variation in  
454 tree size increases total canopy volume occupancy by increasing the number of canopy layers,  
455 but does not necessarily result in a concomitant increase in canopy closure, as the resulting  
456 canopies are often more sparse, due to increased competition for light (Béland & Baldocchi,

457 2021). Both path analyses also support this conclusion, where species diversity was found to  
458 cause an increase in stand structural diversity, but this did not extend to an increase in canopy  
459 closure.

#### 460 4.3 Spatial clustering effects

461 Spatial regularity of stems, measured using the uniform angle index, caused a clear decrease  
462 in canopy closure, with similar behaviour across vegetation types. Uniform angle index was  
463 also included in the best multivariate model predicting canopy closure. Concurrently, spatial  
464 clustering of stems, measured by Voronoi cell area CV was included in the best model for  
465 foliage density but had a positive effect on this canopy complexity metric. This finding is  
466 expected, as spatial clustering results in reduced canopy cover in areas outside clusters, and  
467 a non-compensatory increase in canopy closure within clusters, due to competition among  
468 individuals (Martens et al., 2000). In contrast, changes in spatial regularity of trees do not imply  
469 changes in the distance of stems, only their relative angular positions, though this does generally  
470 correlate with spatial clustering (von Gadow & Hui, 2002).

#### 471 4.4 Plot vs. subplot scale results

472 The standardised effect sizes of species diversity on canopy complexity metrics were generally  
473 greater at the plot level than at the subplot level. While positive and significant relationships  
474 between species diversity and subplot canopy complexity metrics were observed in the subplot  
475 bivariate models, subplot linear mixed effects models did not show strong species diversity effects,  
476 and models were instead dominated by the effect of crowding. This finding suggests a large  
477 degree of stochastic variability in canopy complexity within plots, that can mask species effects at  
478 smaller spatial scales. The prevalence of disturbance events such as fire and damage by elephants  
479 in southern African woodlands (Bond, 2008), as well as tree-fall, small-scale variability in edaphic  
480 factors, and stochastic tree mortality all contribute to heterogeneity in canopy complexity  
481 (Shirima et al., 2015). While disturbances are controlled to some extent by stand structure and  
482 composition, due to the stochastic nature of disturbance events, a snapshot study such as this  
483 cannot capture the average disturbance regime and there is therefore a great deal of noise in  
484 models predicting canopy complexity from species diversity. The contrast in strength of species  
485 diversity effects at the subplot and plot level demonstrates the importance of large sample units,  
486 a high degree of spatial replication, and ideally a longer time scale when measuring canopy  
487 complexity, especially in disturbed systems, to effectively account for inherent heterogeneity in  
488 the system. Even with the one hectare plots used in this study, these plots may still be too small  
489 to fully capture larger scale patch dynamics arising from disturbance feedbacks and edaphic  
490 heterogeneity.

#### 491 4.5 Variation among vegetation types

492 Bivariate relationships showed that some of the observed species diversity effect on canopy closure  
493 and foliage density may be driven by vegetation type, and the variation in species diversity  
494 among vegetation types. The linear mixed model framework however, which accounted for  
495 differences among vegetation types, still shows weak species diversity effects even after vegetation  
496 type is controlled for, strengthening the validity of the result. Canopy complexity metrics  
497 also differed among vegetation types, but significant differences among vegetation types only  
498 occurred in a few cases, mostly between miombo and non-miombo vegetation clusters. Canopy  
499 density and total foliage volume was lowest in ex-Acacia plots, as expected, while the highest  
500 canopy density occurred in miombo plots in Clusters 1 and 2. Miombo woodlands frequently

501 have contiguous canopies with overlapping individual tree canopies (Solbrig et al., 1996), while  
502 ex-Acacia savannas show greater negative density dependence of individuals, forming patchy  
503 canopies with simpler vertical profiles (Pillay & Ward, 2012). From this result it is suggested  
504 that under identical disturbance and climatic regimes, ex-Acacia savannas may not be as effective  
505 at closing their canopy to exclude grasses. Particularly, the lower maximum tree height of trees  
506 in the ex-Acacia plots may preclude these savannas from forming a multi-layer canopy that may  
507 be necessary to allow increased biomass.

508 While vegetation types differed in mean values for stand structural and species diversity metrics,  
509 variation in these metrics produced results of similar direction and magnitude among vegetation  
510 types in most cases where strong effects were observed, suggesting that ecosystem processes  
511 driving canopy complexity are similar, even across these varied savanna types. Small sample  
512 sizes for *Baikiaea* and ex-Acacia vegetation however, led to wide errors on most relationships  
513 especially at the plot level, such that it is impossible to draw deep conclusions about the  
514 behaviour of these vegetation types. Variation in mean values of canopy complexity metrics  
515 among vegetation types is likely driven by species identity and variation in physiological limits  
516 on tree physiognomy (Seidel et al., 2013; Sercu et al., 2017), though species composition itself is  
517 driven by environmental factors and disturbance regime (Ribeiro et al., 2020).

## 518 5 Conclusion

519 Here I explored how tree species diversity and stand structure influence canopy complexity  
520 in southern African savannas, using terrestrial LiDAR methods. I determined that species  
521 diversity causes an increase canopy metrics related to density, and caused separate variation  
522 in tree size and tree density. Together these results suggest that diverse savannas may be able  
523 to upregulate their productivity and more effectively exclude grasses under atmospheric CO<sub>2</sub>  
524 enrichment conditions. The findings presented here have a range of consequences for savanna  
525 land managers that wish to predict future vegetation dynamics, particularly related to woody  
526 encroachment. This study also highlights and compares a number of novel and easy to calculate  
527 metrics for estimating different aspects of canopy complexity using terrestrial LiDAR, and sets a  
528 precedent as one of the few initial studies using terrestrial LiDAR in mesic southern African  
529 savanna landscapes.

## 530 References

- 531 Archibald, S. & W. J. Bond (2003). ‘Growing tall vs growing wide: tree architecture and allometry  
532 of Acacia karroo in forest, savanna, and arid environments’. In: *Oikos* 102.1, pp. 3–14. DOI:  
533 10.1034/j.1600-0706.2003.12181.x.
- 534 Axelsson, C. R. & N. P. Hanan (2018). ‘Rates of woody encroachment in African savannas reflect  
535 water constraints and fire disturbance’. In: *Journal of Biogeography* 45.6, pp. 1209–1218. DOI:  
536 10.1111/jbi.13221.
- 537 Baldocchi, D. D. & K. B. Wilson (2001). ‘Modeling CO<sub>2</sub> and water vapor exchange of a temperate  
538 broadleaved forest across hourly to decadal time scales’. In: *Ecological Modelling* 142.1-2,  
539 pp. 155–184. DOI: 10.1016/s0304-3800(01)00287-3.
- 540 Barry, K. E., L. Mommer, J. van Ruijven, C. Wirth, A. J. Wright, Y. Bai, J. Connolly, G. B. D.  
541 Deyn, H. de Kroon, F. Isbell et al. (2019). ‘The Future of Complementarity: Disentangling  
542 Causes from Consequences’. In: *Trends in Ecology & Evolution* 34.2, pp. 167–180. DOI:  
543 10.1016/j.tree.2018.10.013.

- 544 Béland, M. & D. D. Baldocchi (2021). ‘Vertical structure heterogeneity in broadleaf forests: Effects  
545 on light interception and canopy photosynthesis’. In: *Agricultural and Forest Meteorology* 307,  
546 p. 108525. DOI: 10.1016/j.agrformet.2021.108525.
- 547 Béland, M. & H. Kobayashi (2021). ‘Mapping forest leaf area density from multiview terrestrial  
548 lidar’. In: *Methods in Ecology and Evolution* 12.4, pp. 619–633. DOI: 10.1111/2041-210x.  
549 13550.
- 550 Bond, W. J. (2008). ‘What Limits Trees in C<sub>4</sub> Grasslands and Savannas?’ In: *Annual Review of  
551 Ecology, Evolution, and Systematics* 39.1, pp. 641–659. DOI: 10.1146/annurev.ecolsys.39.  
552 110707.173411.
- 553 Bond, W. J. & G. F. Midgley (2012). ‘Carbon dioxide and the uneasy interactions of trees and  
554 savannah grasses’. In: *Philosophical Transactions of the Royal Society B: Biological Sciences*  
555 367.1588, pp. 601–612. DOI: 10.1098/rstb.2011.0182.
- 556 Buitenwerf, R., W. J. Bond, N. Stevens & W. S. W. Trollope (2012). ‘Increased tree densities  
557 in South African savannas: >50 years of data suggests CO<sub>2</sub> as a driver’. In: *Global Change  
558 Biology* 18.2, pp. 675–684. DOI: 10.1111/j.1365-2486.2011.02561.x.
- 559 Calders, K., J. Adams, J. Armston, H. Bartholomeus, S. Bauwens, L. P. Bentley, J. Chave,  
560 F. M. Danson, M. Demol, M. Disney et al. (2020). ‘Terrestrial laser scanning in forest  
561 ecology: Expanding the horizon’. In: *Remote Sensing of Environment* 251, p. 112102. DOI:  
562 10.1016/j.rse.2020.112102.
- 563 Charles-Dominique, T., G. F. Midgley, K. W. Tomlinson & W. J. Bond (2018). ‘Steal the  
564 light: shade vs fire adapted vegetation in forest-savanna mosaics’. In: *New Phytologist* 218.4,  
565 pp. 1419–1429. DOI: 10.1111/nph.15117.
- 566 Chen, J. M., G. Mo, J. Pisek, J. Liu, F. Deng, M. Ishizawa & D. Chan (2012). ‘Effects of  
567 foliage clumping on the estimation of global terrestrial gross primary productivity’. In: *Global  
568 Biogeochemical Cycles* 26, GB1019. DOI: 10.1029/2010gb003996.
- 569 Cifuentes, R., D. V. der Zande, J. Farifteh, C. Salas & P. Coppin (2014). ‘Effects of voxel size  
570 and sampling setup on the estimation of forest canopy gap fraction from terrestrial laser  
571 scanning data’. In: *Agricultural and Forest Meteorology* 194, pp. 230–240. DOI: 10.1016/j.  
572 agrformet.2014.04.013.
- 573 Criado, M. G., I. H. Myers-Smith, A. D. Bjorkman, C. E. R. Lehmann & N. Stevens (2020).  
574 ‘Woody plant encroachment intensifies under climate change across tundra and savanna biomes’.  
575 In: *Global Ecology and Biogeography* 29.5, pp. 925–943. DOI: 10.1111/geb.13072.
- 576 Devine, A. P., R. A. McDonald, T. Quaife & I. M. D. Maclean (2017). ‘Determinants of  
577 woody encroachment and cover in African savannas’. In: *Oecologia* 183.4, pp. 939–951. DOI:  
578 10.1007/s00442-017-3807-6.
- 579 Dohn, J., D. J. Augustine, N. P. Hanan, J. Ratnam & M. Sankaran (2017). ‘Spatial vegetation  
580 patterns and neighborhood competition among woody plants in an East African savanna’. In:  
581 *Ecology* 98.2, pp. 478–488. DOI: 10.1002/ecy.1659.
- 582 Donohue, R. J., M. L. Roderick, T. R. McVicar & G. D. Farquhar (2013). ‘Impact of CO<sub>2</sub>  
583 fertilization on maximum foliage cover across the globe’s warm, arid environments’. In:  
584 *Geophysical Research Letters* 40.12, pp. 3031–3035. DOI: 10.1002/grl.50563.
- 585 Ehbrecht, M., P. Schall, J. Juchheim, C. Ammer & D. Seidel (2016). ‘Effective number of layers:  
586 A new measure for quantifying three-dimensional stand structure based on sampling with  
587 terrestrial LiDAR’. In: *Forest Ecology and Management* 380, pp. 212–223. DOI: 10.1016/j.  
588 foreco.2016.09.003.
- 589 Fotis, A. T., T. H. Morin, R. T. Fahey, B. S. Hardiman, G. Bohrer & P. S. Curtis (2018).  
590 ‘Forest structure in space and time: Biotic and abiotic determinants of canopy complexity and  
591 their effects on net primary productivity’. In: *Agricultural and Forest Meteorology* 250-251,  
592 pp. 181–191. DOI: 10.1016/j.agrformet.2017.12.251.

- 593 Frost, P. (1996). 'The ecology of miombo woodlands'. In: *The miombo in transition: woodlands*  
594      and welfare in Africa. Ed. by B. Campbell. Bogor, Indonesia: Center for International Forestry  
595      Research, pp. 11–55.
- 596 Getzin, S., T. Wiegand, K. Wiegand & F. He (2008). 'Heterogeneity influences spatial patterns and  
597      demographics in forest stands'. In: *Journal of Ecology* 96.4, pp. 807–820. DOI: 10.1111/j.1365-  
598      2745.2008.01377.x.
- 599 Gough, C. M., J. W. Atkins, R. T. Fahey & B. S. Hardiman (2019). 'High rates of primary  
600      production in structurally complex forests'. In: *Ecology* 100.10. DOI: 10.1002/ecy.2864.
- 601 Groen, T. A. (2007). 'Spatial matters: how spatial processes and patterns affect savanna dynamics'.  
602      PhD thesis. Netherlands.
- 603 Hardiman, B. S., G. Bohrer, C. M. Gough, C. S. Vogel & P. S. Curtis (2011). 'The role of canopy  
604      structural complexity in wood net primary production of a maturing northern deciduous  
605      forest'. In: *Ecology* 92.9, pp. 1818–1827. DOI: 10.1890/10-2192.1.
- 606 Hegyi, F. (1974). 'A simulation model for managing jack-pine stands'. In: *Royal College of  
607      Forestry, editor*. Stockholm, Sweden: Royal College of Forestry, pp. 74–90.
- 608 Hirota, M., M. Holmgren, E. H. Van Nes & M. Scheffer (2011). 'Global resilience of tropical forest  
609      and savanna to critical transitions'. In: *Science* 334, pp. 232–235. DOI: 10.1126/science.  
610      1210657.
- 611 Jonckheere, I., S. Fleck, K. Nackaerts, B. Muys, P. Coppin, M. Weiss & F. Baret (2004). 'Review  
612      of methods for in situ leaf area index determination'. In: *Agricultural and Forest Meteorology*  
613      121.1-2, pp. 19–35. DOI: 10.1016/j.agrformet.2003.08.027.
- 614 Jost, L. (2006). 'Entropy and diversity'. In: *Oikos* 113.2, pp. 363–375. DOI: 10.1111/j.2006.  
615      0030-1299.14714.x.
- 616 Jucker, T., O. Bouriaud & D. A. Coomes (2015). 'Crown plasticity enables trees to optimize  
617      canopy packing in mixed-species forests'. In: *Functional Ecology* 29.8, pp. 1078–1086. DOI:  
618      10.1111/1365-2435.12428.
- 619 Kershaw, J. A., M. J. Ducey, T. W. Beers & B. Husch (2017). *Forest Mensuration*. Chichester,  
620      UK: John Wiley & Sons. ISBN: 9781118902035.
- 621 Khosravipour, A., A. K. Skidmore, M. Isenburg, T. Wang & Y. A. Hussin (2014). 'Generating  
622      Pit-free Canopy Height Models from Airborne LiDAR'. In: *Photogrammetric Engineering &  
623      Remote Sensing* 80.9, pp. 863–872. DOI: 10.14358/pers.80.9.863.
- 624 King, D. A. (1990). 'The Adaptive Significance of Tree Height'. In: *The American Naturalist*  
625      135.6, pp. 809–828. DOI: 10.1086/285075.
- 626 Körner, C. (2017). 'A matter of tree longevity'. In: *Science* 355.6321, pp. 130–131. DOI: 10.1126/  
627      science.aal2449.
- 628 Law, B. E., A. Cescatti & D. D. Baldocchi (2001). 'Leaf area distribution and radiative transfer in  
629      open-canopy forests: implications for mass and energy exchange'. In: *Tree Physiology* 21.12-13,  
630      pp. 777–787. DOI: 10.1093/treephys/21.12-13.777.
- 631 Lefcheck, J. S. (2016). 'piecewiseSEM: Piecewise structural equation modeling in R for ecology,  
632      evolution, and systematics'. In: *Methods in Ecology and Evolution* 7.5, pp. 573–579. DOI:  
633      10.1111/2041-210X.12512.
- 634 Levick, S. R., G. P. Asner, T. Kennedy-Bowdoin & D. E. Knapp (2009). 'The relative influence  
635      of fire and herbivory on savanna three-dimensional vegetation structure'. In: *Biological  
636      Conservation* 142.8, pp. 1693–1700. DOI: 10.1016/j.biocon.2009.03.004.
- 637 Liang, J., T. W. Crowther, N. Picard, S. Wiser, M. Zhou, G. Alberti, E.-D. Schulze, A. D.  
638      McGuire, F. Bozzato, H. Pretzsch et al. (2016). 'Positive biodiversity-productivity relationship  
639      predominant in global forests'. In: *Science* 354, aaf8957-aaf8957. DOI: 10.1126/science.  
640      aaf8957.
- 641 Lowman, M. D. & H. B. Rinker (2004). *Forest Canopies*. Physiological Ecology. Burlington MA,  
642      USA: Elsevier Science. ISBN: 9780080491349.

- 643 Martens, S. N., D. D. Breshears & C. W. Meyer (2000). ‘Spatial distributions of understory  
644 light along the grassland/forest continuum: effects of cover, height, and spatial pattern of tree  
645 canopies’. In: *Ecological Modelling* 126.1, pp. 79–93. DOI: 10.1016/s0304-3800(99)00188-x.
- 646 Mitchard, E. T. A. & C. M. Flintrop (2013). ‘Woody encroachment and forest degradation in  
647 sub-Saharan Africa’s woodlands and savannas 1982-2006’. In: *Philosophical Transactions of the  
648 Royal Society B: Biological Sciences* 368.1625, p. 20120406. DOI: 10.1098/rstb.2012.0406.
- 649 Morin, X. (2015). ‘Species richness promotes canopy packing: a promising step towards a better  
650 understanding of the mechanisms driving the diversity effects on forest functioning’. In:  
651 *Functional Ecology* 29.8, pp. 993–994. DOI: 10.1111/1365-2435.12473.
- 652 Mugasha, W. A., O. M. Bollandsås & T. Eid (2013). ‘Relationships between diameter and height  
653 of trees in natural tropical forest in Tanzania’. In: *Southern Forests: a Journal of Forest  
654 Science* 75.4, pp. 221–237. DOI: 10.2989/20702620.2013.824672.
- 655 Muir, J., S. Phinn, T. Eyre & P. Scarth (2018). ‘Measuring plot scale woodland structure using  
656 terrestrial laser scanning’. In: *Remote Sensing in Ecology and Conservation* 4.4, pp. 320–338.  
657 DOI: 10.1002/rse2.82.
- 658 Muumbe, T. P., J. Baade, J. Singh, C. Schmullius & C. Thau (2021). ‘Terrestrial Laser Scanning  
659 for Vegetation Analyses with a Special Focus on Savannas’. In: *Remote Sensing* 13.3, p. 507.  
660 DOI: 10.3390/rs13030507.
- 661 Nakagawa, S. & I. C. Cuthill (2007). ‘Effect size, confidence interval and statistical significance: a  
662 practical guide for biologists’. In: *Biological Reviews* 82.4, pp. 591–605. DOI: 10.1111/j.1469-  
663 185x.2007.00027.x.
- 664 Ong, M. S., Y. C. Kuang & M. P.-L. Ooi (2012). ‘Statistical measures of two dimensional  
665 point set uniformity’. In: *Computational Statistics & Data Analysis* 56.6, pp. 2159–2181. DOI:  
666 10.1016/j.csda.2011.12.005.
- 667 Panzou, G. J. L., A. Fayolle, T. Jucker, O. L. Phillips, S. Bohlman, L. F. Banin, S. L. Lewis,  
668 K. Affum-Baffoe, L. F. Alves, C. Antin et al. (2020). ‘Pantropical variability in tree crown  
669 allometry’. In: *Global Ecology and Biogeography* 30.2, pp. 459–475. DOI: 10.1111/geb.13231.
- 670 Persistence of Vision Pty. Ltd. (2004). *Persistence of Vision Raytracer (Version 3.7)*. [Computer  
671 software].
- 672 Pillay, T. & D. Ward (2012). ‘Spatial pattern analysis and competition between Acacia karroo  
673 trees in humid savannas’. In: *Plant Ecology* 213.10, pp. 1609–1619. DOI: 10.1007/s11258-  
674 012-0115-4.
- 675 Pilon, N. A. L., G. Durigan, J. Rickenback, R. T. Pennington, K. G. Dexter, W. A. Hoffmann,  
676 R. C. R. Abreu & C. E. R. Lehmann (2020). ‘Shade alters savanna grass layer structure  
677 and function along a gradient of canopy cover’. In: *Journal of Vegetation Science* 32.1. DOI:  
678 10.1111/jvs.12959.
- 679 Plas, F. van der (2019). ‘Biodiversity and ecosystem functioning in naturally assembled com-  
680 munities’. In: *Biological Reviews* 94, pp. 1220–1245. DOI: 10.1111/brv.12499.
- 681 Pretzsch, H. (2014). ‘Canopy space filling and tree crown morphology in mixed-species stands  
682 compared with monocultures’. In: *Forest Ecology and Management* 327, pp. 251–264. DOI:  
683 <http://dx.doi.org/10.1016/j.foreco.2014.04.027>.
- 684 Privette, J., Y. Tian, G. Roberts, R. Scholes, Y. Wang, K. Caylor, P. Frost & M. Mukelabai (2004).  
685 ‘Vegetation structure characteristics and relationships of Kalahari woodlands and savannas’.  
686 In: *Global Change Biology* 10.3, pp. 281–291. DOI: 10.1111/j.1365-2486.2004.00740.x.
- 687 Ratcliffe, S., C. Wirth, T. Jucker, F. van der Plas, M. Scherer-Lorenzen, K. Verheyen, E. Allan,  
688 R. Benavides, H. Bruelheide, B. Ohse et al. (2017). ‘Biodiversity and ecosystem functioning  
689 relations in European forests depend on environmental context’. In: *Ecology Letters* 20,  
690 pp. 1414–1426. DOI: <http://dx.doi.org/10.1111/ele.12849>.
- 691 Reich, P. B., S. E. Hobbie & T. D. Lee (2014). ‘Plant growth enhancement by elevated CO<sub>2</sub>  
692 eliminated by joint water and nitrogen limitation’. In: *Nature Geoscience* 7.12, pp. 920–924.  
693 DOI: 10.1038/ngeo2284.

- 694 Ribeiro, N. S., P. L. Silva de Miranda & J. Timberlake (2020). ‘Biogeography and Ecology  
695 of Miombo Woodlands’. In: *Miombo Woodlands in a Changing Environment: Securing the*  
696 *Resilience and Sustainability of People and Woodlands*. Ed. by N. S. Ribeiro, Y. Katerere,  
697 P. W. Chirwa & I. M. Grundy. Cham, Switzerland: Springer International Publishing, pp. 9–53.  
698 DOI: 10.1007/978-3-030-50104-4\_2.
- 699 Rusu, R. B., Z. C. Marton, N. Blodow, M. Dolha & M. Beetz (2008). ‘Towards 3D Point cloud  
700 based object maps for household environments’. In: *Robotics and Autonomous Systems* 56.11,  
701 pp. 927–941. DOI: 10.1016/j.robot.2008.08.005.
- 702 Sankaran, M., N. P. Hanan, R. J. Scholes, J. Ratnam, D. J. Augustine, B. S. Cade, J. Gignoux,  
703 S. I. Higgins, X. Le Roux, F. Ludwig et al. (2005). ‘Determinants of woody cover in African  
704 savannas’. In: *Nature* 438.8, pp. 846–849. DOI: <http://dx.doi.org/10.1038/nature04070>.
- 705 Schertzer, E., A. C. Staver & S. A. Levin (2015). ‘Implications of the spatial dynamics of fire  
706 spread for the bistability of savanna and forest’. In: *Journal of Mathematical Biology* 70.1–2,  
707 pp. 329–341. DOI: 10.1007/s00285-014-0757-z.
- 708 Scheuermann, C. M., L. E. Nave, R. T. Fahey, K. J. Nadelhoffer & C. M. Gough (2018). ‘Effects  
709 of canopy structure and species diversity on primary production in upper Great Lakes forests’.  
710 In: *Oecologia* 188.2, pp. 405–415. DOI: 10.1007/s00442-018-4236-x.
- 711 Scholes, R. J. & S. R. Archer (1997). ‘Tree grass interactions in savannas’. In: *Annual Review of  
712 Ecology and Systematics*.
- 713 Seidel, D., S. Fleck & C. Leuschner (2012). ‘Analyzing forest canopies with ground-based  
714 laser scanning: A comparison with hemispherical photography’. In: *Agricultural and Forest  
715 Meteorology* 154–155, pp. 1–8. DOI: 10.1016/j.agrformet.2011.10.006.
- 716 Seidel, D., C. Leuschner, C. Scherber, F. Beyer, T. Wommelsdorf, M. J. Cashman & L. Fehrmann  
717 (2013). ‘The relationship between tree species richness, canopy space exploration and  
718 productivity in a temperate broad-leaf mixed forest’. In: *Forest Ecology and Management* 310,  
719 pp. 366–374. DOI: 10.1016/j.foreco.2013.08.058.
- 720 Sercu, B. K., L. Baeten, F. van Coillie, A. Martel, L. Lens, K. Verheyen & D. Bonte (2017).  
721 ‘How tree species identity and diversity affect light transmittance to the understory in mature  
722 temperate forests’. In: *Ecology and Evolution* 7.24, pp. 10861–10870. DOI: 10.1002/ece3.3528.
- 723 Shenkin, A., L. P. Bentley, I. Oliveras, N. Salinas, S. Adu-Bredu, B. H. Marimon-Junior, B. S.  
724 Marimon, T. Peprah, E. L. Choque, L. T. Rodriguez et al. (2020). ‘The Influence of Ecosystem  
725 and Phylogeny on Tropical Tree Crown Size and Shape’. In: *Frontiers in Forests and Global  
726 Change* 3. DOI: 10.3389/ffgc.2020.501757.
- 727 Shirima, D. D., M. Pfeifer, P. J. Platts, Ø. Totland & S. R. Moe (2015). ‘Interactions between  
728 Canopy Structure and Herbaceous Biomass along Environmental Gradients in Moist Forest  
729 and Dry Miombo Woodland of Tanzania’. In: *PLOS ONE* 10.11, e0142784. DOI: 10.1371/  
730 journal.pone.0142784.
- 731 Silva, I. A. & M. A. Batalha (2011). ‘Plant functional types in Brazilian savannas: The niche par-  
732 titioning between herbaceous and woody species’. In: *Perspectives in Plant Ecology, Evolution  
733 and Systematics* 13.3, pp. 201–206. DOI: 10.1016/j.ppees.2011.05.006.
- 734 Sitch, S., P. Friedlingstein, N. Gruber, S. D. Jones, G. Murray-Tortarolo, A. Ahlström, S. C.  
735 Doney, H. Graven, C. Heinze, C. Huntingford et al. (2015). ‘Recent trends and drivers of  
736 regional sources and sinks of carbon dioxide’. In: *Biogeosciences* 12.3, pp. 653–679. DOI:  
737 10.5194/bg-12-653-2015.
- 738 Solbrig, O. T., E. Medina & J. F. Silva (1996). *Biodiversity and Savanna Ecosystem Processes*.  
739 Berlin, Germany: Springer-Verlag.
- 740 Stark, S. C., B. J. Enquist, S. R. Saleska, V. Leitold, J. Schietti, M. Longo, L. F. Alves, P. B.  
741 Camargo & R. C. Oliveira (2015). ‘Linking canopy leaf area and light environments with tree  
742 size distributions to explain Amazon forest demography’. In: *Ecology Letters* 18.7, pp. 636–645.  
743 DOI: 10.1111/ele.12440.

- 744 Staver, A. C. & S. E. Koerner (2015). ‘Top-down and bottom-up interactions determine tree  
 745 and herbaceous layer dynamics in savanna grasslands’. In: *Trophic Ecology: Bottom-up and*  
 746 *Top-Down Interactions Across Aquatic and Terrestrial Systems*. Ed. by K. J. La Pierre &  
 747 T. C. Hanley. Cambridge, United Kingdom: Cambridge University Press, pp. 86–106.
- 748 Stevens, N., C. E. R. Lehmann, B. P. Murphy & G. Durigan (2016). ‘Savanna woody encroachment  
 749 is widespread across three continents’. In: *Global Change Biology* 23.1, pp. 235–244. DOI:  
 750 10.1111/gcb.13409.
- 751 ter Steege, H. (2018). *Hemiphot.R: Free R scripts to analyse hemispherical photographs for*  
 752 *canopy openness, leaf area index and photosynthetic active radiation under forest canopies*.  
 753 Unpublished report. Leiden, The Netherlands: Naturalis Biodiversity Center. URL: <https://github.com/Naturalis/Hemiphot>.
- 755 von Gadow, K. & G. Hui (2002). *Characterising forest spatial structure and diversity*. Ed. by  
 756 L. Bjoerk. Lund, Sweden, pp. 20–30.
- 757 Wakeling, J. L., A. C. Staver & W. J. Bond (2011). ‘Simply the best: the transition of savanna  
 758 saplings to trees’. In: *Oikos* 120.10, pp. 1448–1451. DOI: 10.1111/j.1600-0706.2011.19957.  
 759 x.
- 760 White, F. (1983). *The Vegetation of Africa: A descriptive memoir to accompany the UNESCO/AETFAT/UNSO vegetation map of Africa*. Paris, France: UNESCO. DOI: 10.2307/  
 761 2260340.
- 763 Wright, A. J., W. D. A. Wardle, W. R. Callaway & A. Gaxiola (2017). ‘The overlooked role of  
 764 facilitation in biodiversity experiments’. In: *Trends in Ecology & Evolution* 32, pp. 383–390.  
 765 DOI: 10.1016/j.tree.2017.02.011.
- 766 Zhang, K., S.-C. Chen, D. Whitman, M.-L. Shyu, J. Yan & C. Zhang (2003). ‘A progressive  
 767 morphological filter for removing nonground measurements from airborne LIDAR data’. In:  
 768 *IEEE Transactions on Geoscience and Remote Sensing* 41.4, pp. 872–882. DOI: 10.1109/tgrs.  
 769 2003.810682.

Table 6: Summary statistics of bivariate linear models comparing canopy complexity metrics with diversity and stand structural metrics, grouped by vegetation type. Note that models plot level canopy complexity metrics could not be fitted for Cluster 4, as this cluster only contained two plots. Slope refers to the slope of the predictor term in the model,  $\pm 1$  standard error. T is the t-value of the slope of the predictor term in the model, Asterisks indicate the p-value of these terms (\*\*\*<0.001, \*\*<0.01, \*<0.05).

Response	Predictor	Cluster	Slope	F	R <sup>2</sup>	T
Foliage density	Basal area CV	1	7.3e+01 $\pm$ 3.7e+01	4.0(2,97)	0.04	1.99*
		2	1.1e+02 $\pm$ 7.9e+01	2.1(2,38)	0.05	1.44
		3	1.4e+01 $\pm$ 7.2e+01	0.0(2,14)	0.00	0.20
		4	1.6e+01 $\pm$ 2.0e+02	0.0(2,12)	0.00	0.08
Foliage density	Hegyi	1	5.9e+03 $\pm$ 2.1e+03	8.2(2,102)	0.07	2.86**
		2	1.4e+04 $\pm$ 3.6e+03	15.2(2,40)	0.28	3.90***
		3	6.6e+03 $\pm$ 3.0e+03	4.8(2,23)	0.17	2.18*
		4	1.5e+01 $\pm$ 5.5e+03	0.0(2,13)	0.00	0.00
Foliage density	Shannon	1	2.2e+03 $\pm$ 1.3e+03	2.8(2,102)	0.03	1.67
		2	3.8e+03 $\pm$ 2.4e+03	2.6(2,39)	0.06	1.61
		3	1.1e+04 $\pm$ 6.5e+03	3.1(2,20)	0.13	1.77
		4	-6.5e+03 $\pm$ 6.5e+03	1.0(2,13)	0.07	-1.01
Canopy closure	Basal area CV	1	1.7e-04 $\pm$ 6.0e-04	0.1(2,97)	0.00	0.28
		2	2.9e-03 $\pm$ 1.1e-03	6.9(2,39)	0.15	2.62*

		3	4.2e-03±1.1e-03	15.1(2,14)	0.52	3.89**
		4	-4.6e-03±3.0e-03	2.2(2,12)	0.16	-1.50
Canopy closure	Hegyi	1	2.2e-01±2.8e-02	62.3(2,102)	0.38	7.89***
		2	2.6e-01±5.1e-02	27.0(2,41)	0.40	5.19***
		3	2.8e-01±4.0e-02	50.7(2,23)	0.69	7.12***
		4	1.7e-01±8.0e-02	4.5(2,13)	0.26	2.12
Canopy closure	Shannon	1	3.1e-03±2.2e-02	0.0(2,102)	0.00	0.14
		2	1.1e-01±3.2e-02	12.1(2,40)	0.23	3.48**
		3	2.3e-01±1.4e-01	2.9(2,20)	0.13	1.69
		4	6.7e-02±1.1e-01	0.4(2,13)	0.03	0.60
Foliage uniformity	Basal area CV	1	3.7e+00±4.0e+00	0.9(2,97)	0.01	0.92
		2	4.5e+00±7.4e+00	0.4(2,38)	0.01	0.61
		3	-3.5e+00±5.9e+00	0.4(2,14)	0.02	-0.59
		4	-9.3e-01±1.5e+01	0.0(2,12)	0.00	-0.06
Foliage uniformity	Hegyi	1	2.2e+02±2.3e+02	1.0(2,102)	0.01	0.98
		2	7.5e+02±3.7e+02	4.0(2,40)	0.09	2.00
		3	4.5e+02±2.6e+02	2.9(2,23)	0.11	1.72
		4	-7.5e+01±4.0e+02	0.0(2,13)	0.00	-0.19
Foliage uniformity	Shannon	1	2.3e+02±1.4e+02	2.6(2,102)	0.02	1.61
		2	8.6e+01±2.2e+02	0.1(2,39)	0.00	0.38
		3	1.3e+03±5.1e+02	6.1(2,20)	0.23	2.48*
		4	-5.9e+02±4.7e+02	1.6(2,13)	0.11	-1.27
Layer diversity	Basal area CV	1	2.5e-02±9.3e-03	7.1(2,97)	0.07	2.66**
		2	3.9e-02±1.4e-02	8.0(2,38)	0.17	2.83**
		3	2.7e-02±2.3e-02	1.3(2,14)	0.09	1.15
		4	2.1e-02±3.1e-02	0.5(2,12)	0.04	0.67
Layer diversity	Hegyi	1	2.7e+00±4.9e-01	29.1(2,102)	0.22	5.39***
		2	2.0e+00±7.5e-01	7.1(2,40)	0.15	2.66*
		3	1.9e+00±1.0e+00	3.6(2,23)	0.13	1.89
		4	1.1e+00±8.5e-01	1.8(2,13)	0.12	1.33
Layer diversity	Shannon	1	1.0e+00±3.4e-01	8.7(2,102)	0.08	2.95**
		2	9.5e-01±4.3e-01	4.8(2,39)	0.11	2.18*
		3	4.9e+00±1.8e+00	7.2(2,20)	0.26	2.68*
		4	1.8e-01±1.1e+00	0.0(2,13)	0.00	0.16
Canopy roughness	Basal area CV	1	1.2e-01±6.9e-02	2.9(2,6)	0.33	1.72
		2	-3.2e-01±2.9e-01	1.2(2,3)	0.29	-1.10
		3	3.5e-01±4.7e-01	0.6(2,1)	0.36	0.74
		4				
Canopy roughness	Voronoi CV	1	2.6e-01±1.2e+00	0.0(2,6)	0.01	0.22
		2	4.6e+00±1.9e+00	6.1(2,3)	0.67	2.48
		3	1.8e+00±1.9e+00	1.0(2,1)	0.49	0.99
		4				
Canopy roughness	Mingling	1	-4.2e+01±5.7e+01	0.5(2,6)	0.08	-0.74
		2	1.6e+01±9.7e+01	0.0(2,3)	0.01	0.17
		3	3.5e+02±2.5e+02	2.0(2,1)	0.67	1.42
		4				

Canopy roughness	Tree density	1	-4.3e-02±4.5e-02	0.9(2,6)	0.13 -0.96
		2	-5.9e-02±3.1e-02	3.6(2,3)	0.54 -1.89
		3	-1.8e-01±2.6e-01	0.5(2,1)	0.31 -0.68
		4			
Canopy roughness	Shannon	1	-2.3e+00±1.7e+00	1.7(2,6)	0.22 -1.32
		2	-1.4e+00±2.4e+00	0.4(2,3)	0.11 -0.60
		3	3.4e+01±4.7e+01	0.5(2,1)	0.34 0.72
		4			
Canopy roughness	Uniform angle index	1	-7.4e+01±2.6e+02	0.1(2,6)	0.01 -0.28
		2	4.1e+02±9.5e+02	0.2(2,3)	0.06 0.43
		3	4.4e+02±5.7e+02	0.6(2,1)	0.37 0.76
		4			
Canopy height	Basal area CV	1	-6.5e-03±6.1e-03	1.1(2,6)	0.16 -1.07
		2	4.3e-02±4.0e-02	1.2(2,3)	0.28 1.08
		3	-3.1e-02±8.7e-03	12.3(2,1)	0.92 -3.51
		4			
Canopy height	Voronoi CV	1	-1.0e-01±8.6e-02	1.5(2,6)	0.20 -1.21
		2	-7.0e-01±2.0e-01	12.7(2,3)	0.81 -3.57*
		3	-1.8e-02±1.4e-01	0.0(2,1)	0.02 -0.13
		4			
Canopy height	Mingling	1	6.8e+00±3.8e+00	3.2(2,6)	0.34 1.78
		2	-3.3e+00±1.3e+01	0.1(2,3)	0.02 -0.25
		3	-2.3e+01±9.3e-01	619.2(2,1)	1.00 -24.88*
		4			
Canopy height	Tree density	1	-3.5e-04±3.8e-03	0.0(2,6)	0.00 -0.09
		2	8.6e-03±4.0e-03	4.7(2,3)	0.61 2.16
		3	-1.0e-03±1.7e-02	0.0(2,1)	0.00 -0.06
		4			
Canopy height	Shannon	1	2.8e-01±1.1e-01	7.1(2,6)	0.54 2.66*
		2	1.7e-01±3.3e-01	0.3(2,3)	0.08 0.52
		3	-3.0e+00±9.0e-01	11.1(2,1)	0.92 -3.32
		4			
Canopy height	Uniform angle index	1	1.0e+01±2.1e+01	0.2(2,6)	0.04 0.49
		2	-7.2e+01±1.3e+02	0.3(2,3)	0.09 -0.56
		3	6.0e-02±3.9e+01	0.0(2,1)	0.00 0.00
		4			
Canopy closure	Basal area CV	1	3.6e-04±6.9e-04	0.3(2,10)	0.03 0.53
		2	3.5e-03±3.5e-03	1.0(2,3)	0.24 0.98
		3	1.9e-03±5.3e-03	0.1(2,1)	0.11 0.35
		4			
Canopy closure	Voronoi CV	1	9.3e-03±8.2e-03	1.3(2,10)	0.11 1.13
		2	-6.6e-02±7.9e-03	69.7(2,3)	0.96 -8.35**
		3	-2.5e-02±4.6e-03	29.0(2,1)	0.97 -5.39
		4			
Canopy closure	Mingling	1	-1.6e-01±5.1e-01	0.1(2,10)	0.01 -0.31
		2	-6.9e-01±1.1e+00	0.4(2,3)	0.12 -0.63
		3	7.6e-02±4.1e+00	0.0(2,1)	0.00 0.02

4					
Canopy closure	Tree density	1	1.4e-04±4.0e-04	0.1(2,10)	0.01 0.36
		2	8.5e-04±2.4e-04	12.2(2,3)	0.80 3.50*
		3	3.0e-03±4.3e-06	499683.9(2,1)	1.00 706.88***
		4			
Canopy closure	Shannon	1	-7.6e-03±1.7e-02	0.2(2,10)	0.02 -0.45
		2	8.5e-03±3.0e-02	0.1(2,3)	0.03 0.28
		3	1.9e-01±5.2e-01	0.1(2,1)	0.12 0.37
		4			
Canopy closure	Uniform angle index	1	-3.9e+00±2.3e+00	2.9(2,10)	0.23 -1.71
		2	-1.2e+01±9.3e+00	1.7(2,3)	0.36 -1.30
		3	-6.9e+00±3.9e-01	306.2(2,1)	1.00 -17.50*
		4			
Foliage density	Basal area CV	1	-4.5e+01±2.9e+01	2.3(2,6)	0.28 -1.52
		2	1.5e+02±1.4e+02	1.1(2,3)	0.27 1.05
		3	1.8e+02±8.9e+01	4.2(2,1)	0.81 2.06
		4			
Foliage density	Voronoi CV	1	3.5e+01±5.0e+02	0.0(2,6)	0.00 0.07
		2	-7.7e+02±1.5e+03	0.3(2,3)	0.08 -0.51
		3	2.7e+02±8.7e+02	0.1(2,1)	0.09 0.31
		4			
Foliage density	Mingling	1	4.5e+03±2.5e+04	0.0(2,6)	0.01 0.18
		2	8.0e+02±4.7e+04	0.0(2,3)	0.00 0.02
		3	1.5e+05±2.0e+04	54.1(2,1)	0.98 7.35
		4			
Foliage density	Tree density	1	8.8e+00±2.0e+01	0.2(2,6)	0.03 0.45
		2	1.1e+01±2.1e+01	0.3(2,3)	0.08 0.51
		3	-1.3e+01±1.1e+02	0.0(2,1)	0.01 -0.12
		4			
Foliage density	Shannon	1	2.5e+02±8.1e+02	0.1(2,6)	0.02 0.31
		2	5.0e+02±1.2e+03	0.2(2,3)	0.05 0.42
		3	1.8e+04±9.1e+03	3.9(2,1)	0.80 1.98
		4			
Foliage density	Uniform angle index	1	-1.1e+05±1.0e+05	1.3(2,6)	0.18 -1.15
		2	1.2e+05±4.7e+05	0.1(2,3)	0.02 0.25
		3	4.3e+04±2.5e+05	0.0(2,1)	0.03 0.18
		4			
Canopy rugosity	Basal area CV	1	-1.0e-01±6.1e-01	0.0(2,6)	0.00 -0.17
		2	-2.2e+00±2.2e+00	1.1(2,3)	0.26 -1.03
		3	8.7e+00±5.4e+00	2.6(2,1)	0.73 1.62
		4			
Canopy rugosity	Voronoi CV	1	7.9e+00±8.2e+00	0.9(2,6)	0.13 0.96
		2	3.5e+01±1.3e+01	6.8(2,3)	0.69 2.61
		3	1.8e+01±4.2e+01	0.2(2,1)	0.15 0.42
		4			
1 -5.9e+02±3.6e+02 2.7(2,6) 0.31 -1.63					
Canopy rugosity	Mingling				

		2	$8.5e+02 \pm 5.2e+02$	$2.7(2,3)$	0.47	1.63
		3	$7.2e+03 \pm 1.7e+03$	$17.6(2,1)$	0.95	4.19
		4				
Canopy rugosity	Tree density	1	$-1.9e-01 \pm 3.4e-01$	$0.3(2,6)$	0.05	-0.56
		2	$-4.6e-01 \pm 2.1e-01$	$4.9(2,3)$	0.62	-2.22
		3	$-1.2e+00 \pm 5.4e+00$	$0.0(2,1)$	0.05	-0.22
		4				
Canopy rugosity	Shannon	1	$-2.4e+01 \pm 1.0e+01$	$5.3(2,6)$	0.47	-2.31
		2	$6.4e+00 \pm 1.8e+01$	$0.1(2,3)$	0.04	0.35
		3	$8.5e+02 \pm 5.4e+02$	$2.5(2,1)$	0.71	1.57
		4				
Canopy rugosity	Uniform angle index	1	$-2.6e+03 \pm 1.6e+03$	$2.5(2,6)$	0.30	-1.58
		2	$1.0e+04 \pm 4.1e+03$	$6.1(2,3)$	0.67	2.47
		3	$3.4e+03 \pm 1.2e+04$	$0.1(2,1)$	0.07	0.28
		4				

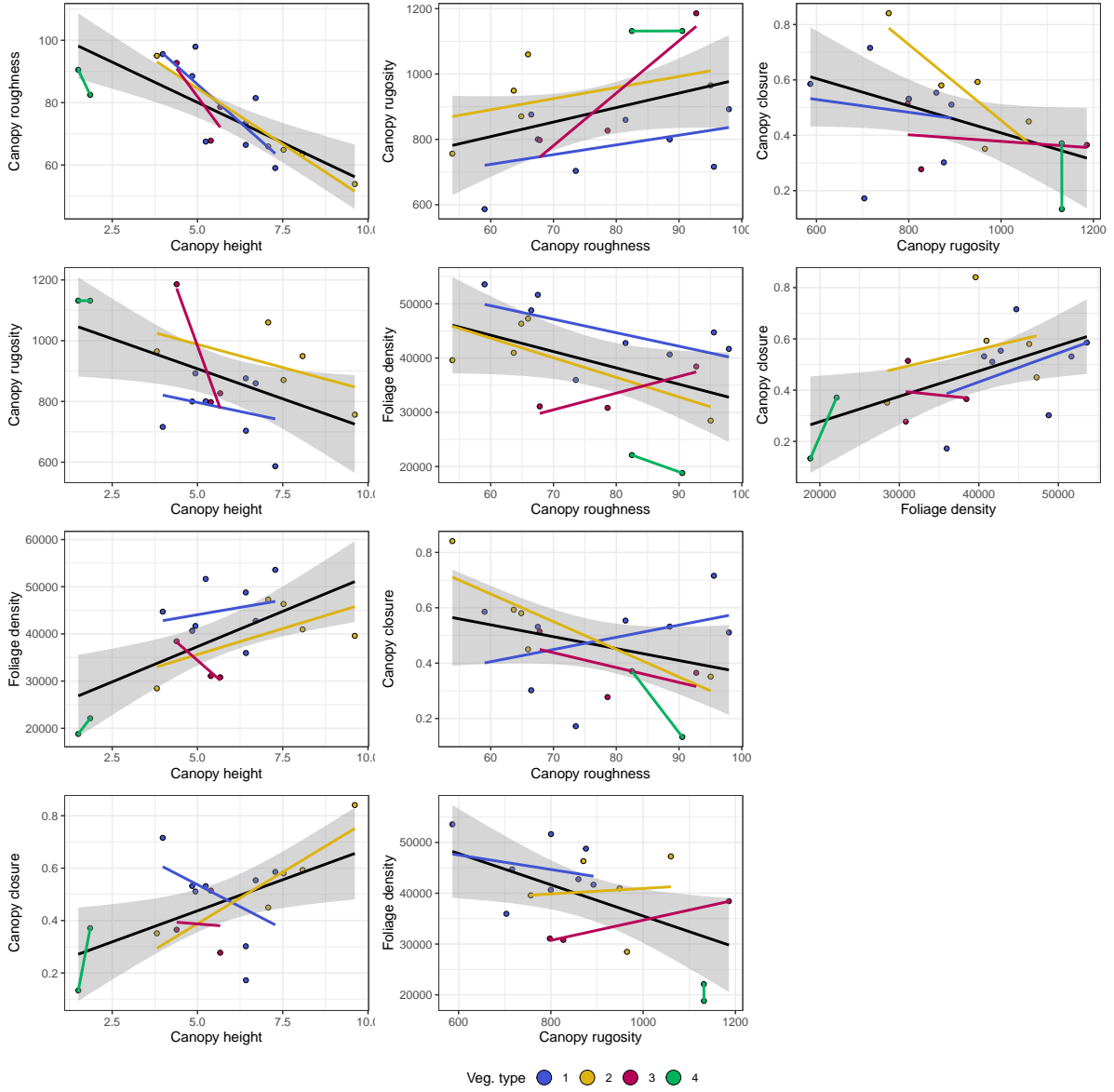


Figure 12: Bivariate scatter plots of plot level canopy complexity metrics.

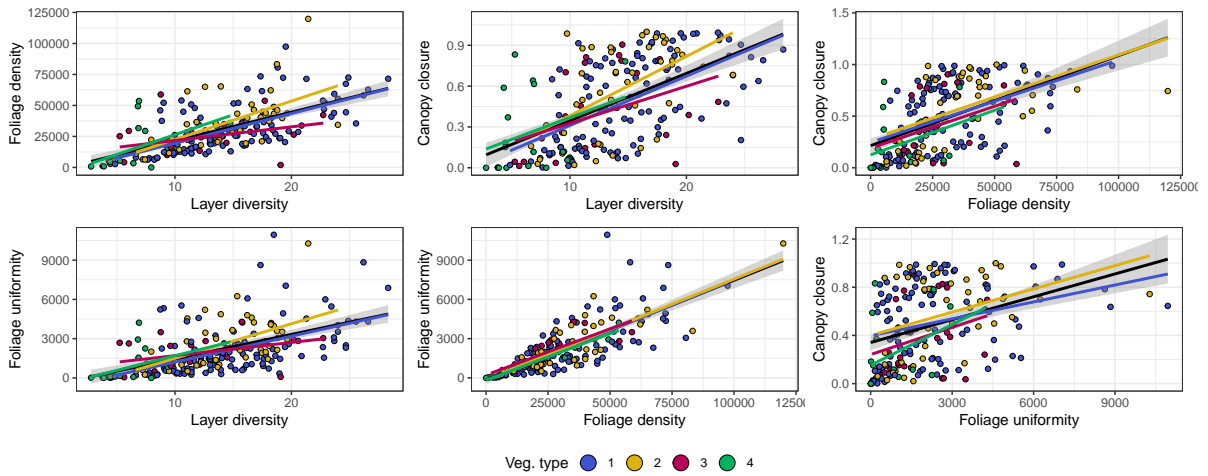


Figure 13: Bivariate scatter plots of subplot level canopy complexity metrics.

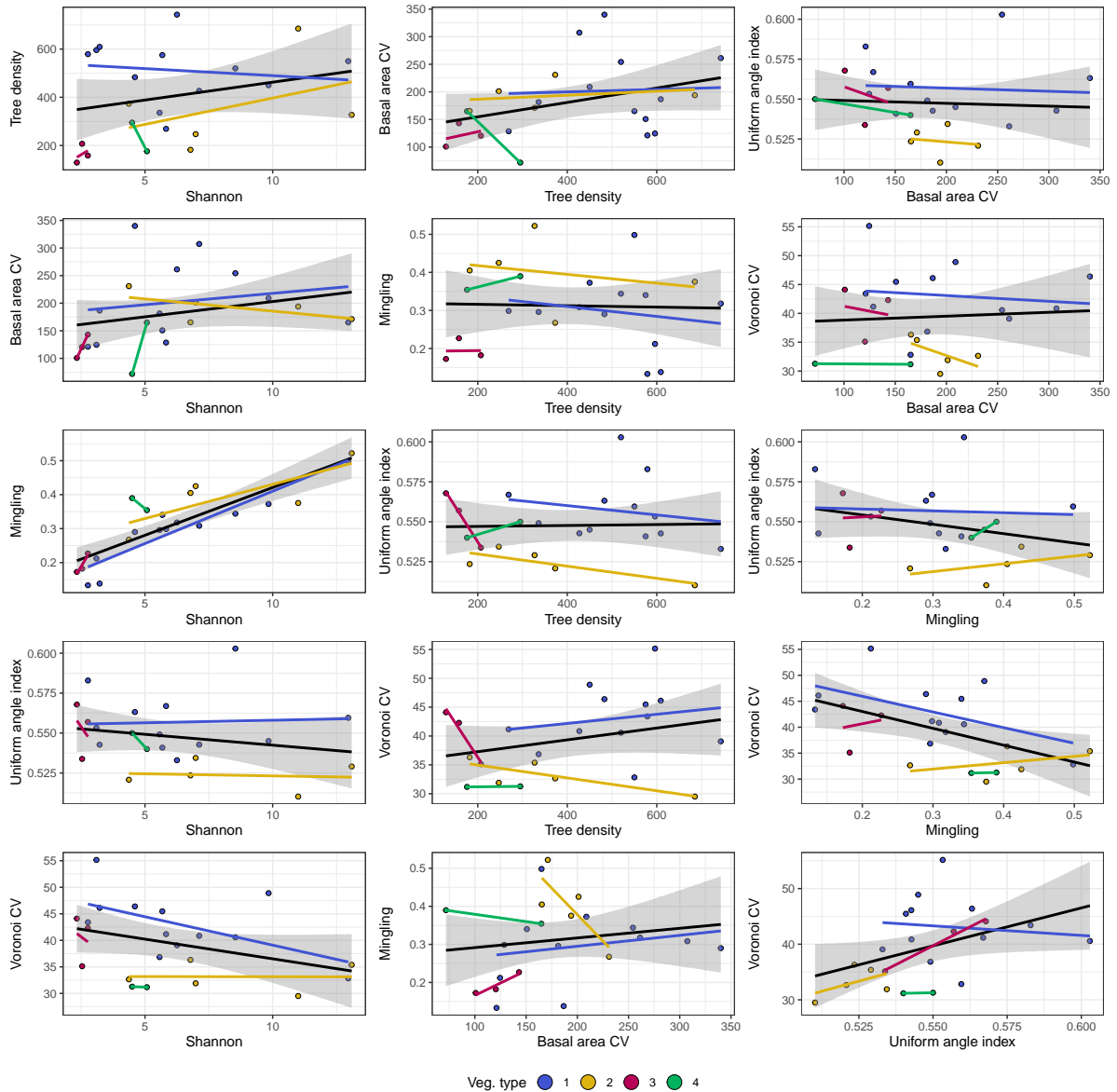


Figure 14: Bivariate scatter plots of plot level diversity and stand structural metrics.

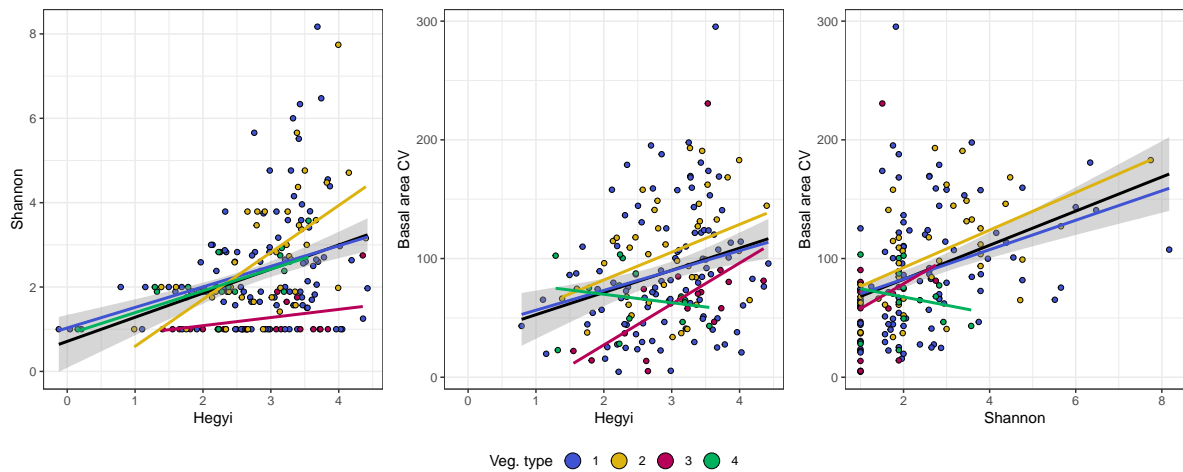


Figure 15: Bivariate scatter plots of subplot level diversity and stand structural metrics.

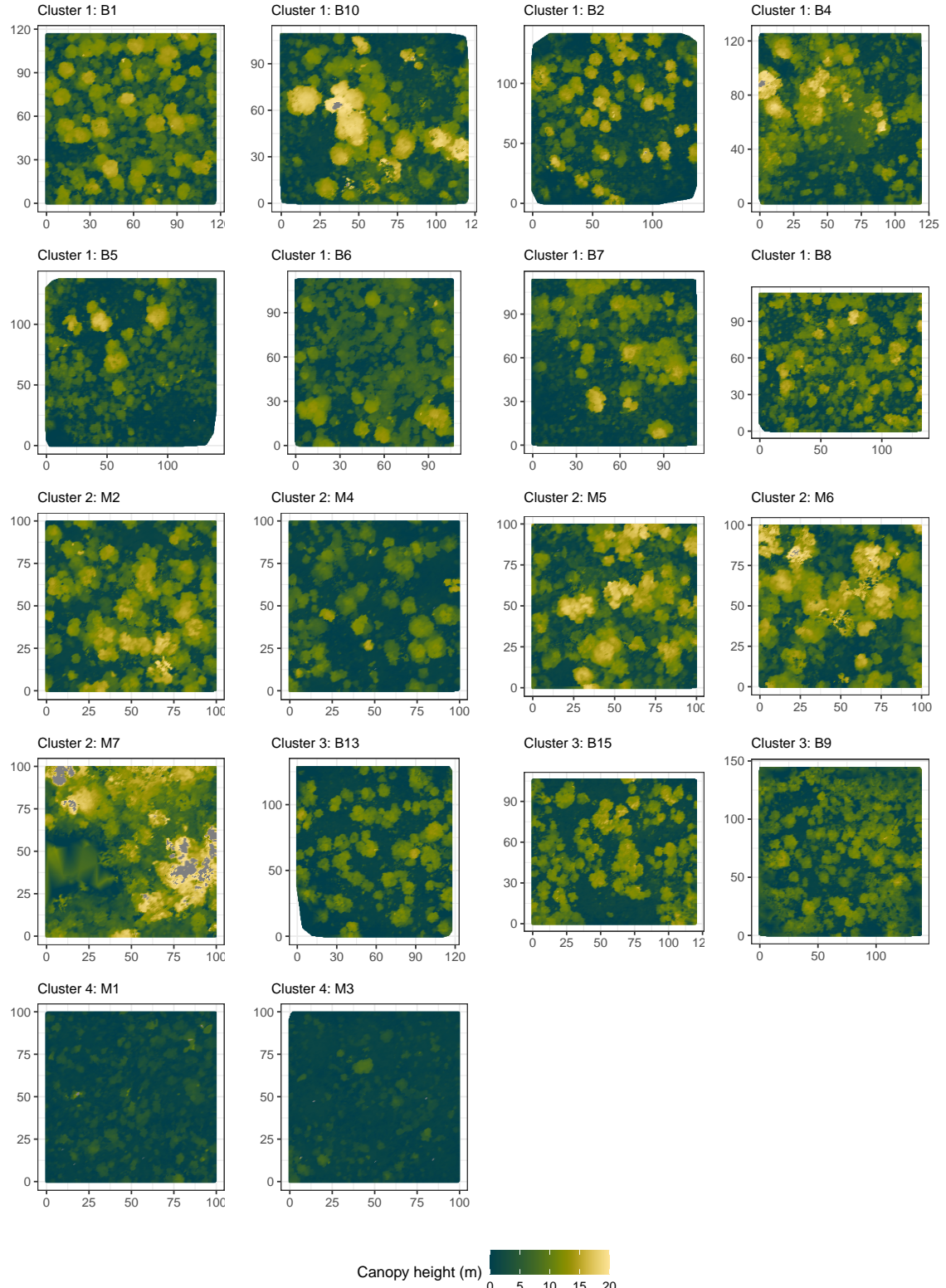


Figure 16: Bivariate scatter plots of subplot level diversity and stand structural metrics.